Decarbonizing the steel industry : techno-economic assessement and modeling of electric arc furnace (en ce compris une introduction à la méthodologie de la recherche

Auteur : Massau, Lisa
Promoteur(s) : Léonard, Grégoire
Faculté : Faculté des Sciences appliquées
Diplôme : Master : ingénieur civil en chimie et science des matériaux, à finalité spécialisée en Chemical Engineering
Année académique : 2025-2026
URI/URL : http://hdl.handle.net/2268.2/26138

UNIVERSITY OF LIEGE
FACULTY OF APPLIED SCIENCE

Decarbonizing the steel industry : techno-economic assessement and modeling of electric arc furnace

Massau Lisa

Thesis presented to obtain the degree of :
Master of Science in Chemical Engineering

Thesis supervisor :
Léonard Grégoire

Academic year: **2025 - 2026**

Acknowledgments

First and foremost, I would like to express my sincere gratitude to my supervisor, Professor Léonard Grégoire. I thank him for accepting to supervise this Master's thesis on such short notice. I am deeply grateful for his continuous help and guidance throughout this project. His insightful feedback constantly pushed me to think further and improve this work.

My special thanks go to Rafailia Mitraki who followed and supported me the most during the realization of this thesis. Her daily help is what allowed me to complete this work, and I also warmly thank her for her invaluable assistance in proofreading this report.

I am also deeply thankful to Vincent Piret, Valentin Sampoux and Fabrice Van Meerhaeghe from APERAM Châtelet for generously sharing their time and expertise. Their insights were essential in helping me understand the process and in selecting the most appropriate data to accurately represent it.

Furthermore, I wish to acknowledge the IPESE group of EPFL for granting me the opportunity to work with the software they developed to build my model.

Finally, I would like to thank my family and all the friends I have met during my studies. They shared both the good and the bad times with me and allowed me to keep so many good memories. Above all, I give a massive thank you to my parents: without you, I would never have been able to make it this far.

Abstract

The steel industry is responsible for approximately 7% of global CO_2 emissions, making its decarbonization a critical challenge in the pursuit of carbon neutrality by 2050. Among the available steelmaking routes, the electric arc furnace (EAF) represents one of the least carbon-intensive technologies, relying primarily on recycled scrap as raw material. This thesis presents a techno-economic assessment of stainless steel production via EAF, with a focus on modelling alternative pathways to further reduce its environmental impact.

The production process considered consists of three main steps: the electric arc furnace, the argon oxygen decarbonizer (AOD), and continuous casting followed by hot rolling. Each step was modelled using a black-box approach, with mass and energy balances derived from literature. The modelling framework used is OSMOSE, a Lua-based multi-objective optimization tool developed by the IPESE group at EPFL. Five configurations were investigated and compared: the conventional natural gas-based process (NG), natural gas with carbon capture (NG+CC), biomethane substitution (BIOCH4), biomethane with carbon capture (BIOCH4+CC), and hydrogen substitution (H2). Three energy price scenarios were considered: a current 2026 scenario, an optimistic ideal scenario, and a competition scenario as well as two emission factor contexts reflecting current and projected 2050 electricity mixes.

Results show that fuel switching to biomethane reduces scope 1 emissions by 37% compared to the base case, while the addition of carbon capture using monoethanolamine (MEA) absorption achieves reductions of up to 93% when combined with biomethane. From an economic standpoint, the natural gas configuration remains the cheapest in most scenarios, as raw material costs dominate the total cost structure. Biomethane emerges as the most promising near-term alternative, offering a favourable balance between emission reductions and cost, particularly under the ideal pricing scenario. Hydrogen shows potential in future scenarios where its production cost decreases significantly, but remains limited today by both cost and availability constraints. Carbon capture technologies, while highly effective in reducing direct emissions, are penalized by their high energy consumption and associated fuel costs, rendering them economically unattractive under current and near-future conditions.

This study provides a decision-support framework for the EAF stainless steel industry and highlights that the economic viability of decarbonization pathways is highly sensitive to future energy price evolution and the availability of renewable fuels.

Résumé

L'industrie sidérurgique est responsable d'environ 7% des émissions mondiales de CO_2, faisant de sa décarbonation un défi majeur dans la poursuite de la neutralité carbone d'ici 2050. Parmi les différentes voies de production d'acier existantes, le four à arc électrique (EAF) représente l'une des technologies les moins émettrices en carbone, reposant principalement sur de la ferraille recyclée comme matière première. Ce travail de fin d'études présente une évaluation technico-économique de la production d'acier inoxydable par EAF, en s'intéressant à la modélisation de voies alternatives permettant de réduire davantage son impact environnemental.

Le procédé de production étudié comprend trois étapes principales : le four à arc électrique, le convertisseur argon-oxygène (AOD) et la coulée continue suivie du laminage à chaud. Chaque étape a été modélisée à l'aide d'une approche boîte noire, avec des bilans de masse et d'énergie issus de la littérature. L'outil de modélisation utilisé est OSMOSE, un logiciel d'optimisation multi-objectifs développé par le groupe IPESE de l'EPFL. Cinq configurations ont été étudiées et comparées : le procédé conventionnel au gaz naturel (NG), le gaz naturel avec capture de carbone (NG+CC), la substitution par du biométhane (BIOCH4), le biométhane avec capture de carbone (BIOCH4+CC), et la substitution par de l'hydrogène (H2). Trois scénarios de prix de l'énergie ont été considérés : un scénario actuel 2026, un scénario idéal optimiste et un scénario compétitif ainsi que deux contextes de facteurs d'émission reflétant respectivement les mix électriques actuels et projetés à l'horizon 2050.

Les résultats montrent que la substitution du gaz naturel par du biométhane permet de réduire les émissions de scope 1 de 37% par rapport au cas de référence, tandis que l'ajout d'une unité de capture du carbone par absorption à la monoéthanolamine (MEA) permet d'atteindre des réductions allant jusqu'à 93% en combinaison avec le biométhane. D'un point de vue économique, la configuration au gaz naturel reste la moins coûteuse dans la plupart des scénarios, les coûts des matières premières dominant la structure de coût totale. Le biométhane apparaît comme l'alternative la plus prometteuse à court terme, offrant un équilibre favorable entre réduction des émissions et coût de production, en particulier dans le scénario de prix idéal. L'hydrogène présente un potentiel intéressant dans les scénarios futurs où son coût de production diminue significativement, mais reste aujourd'hui limité par des contraintes à la fois économiques et de disponibilité. Les technologies de capture du carbone, bien qu'efficaces pour réduire les émissions directes, sont pénalisées par leur forte consommation énergétique et les coûts en combustible associés, les rendant peu attractives économiquement dans les conditions actuelles et à court terme. Cette étude fournit un outil d'aide à la décision pour l'industrie sidérurgique utilisant le four à arc électrique et souligne que la viabilité économique des voies de décarbonation est fortement sensible à l'évolution future des prix de l'énergie et à la disponibilité des combustibles renouvelables.

Contents

List of Figures

List of Tables

List of acronyms

AOD Argon Oxygen Decarbonization
BF Blast Furnace
BIOCH4 Biomethane
BOF Blast Oxygen Furnace
CC Carbone Capture
DRI Direct Reduction Iron
EAF Electric Arc Furnace
HBI Hot Briquetted Iron
NG Natural Gas
PCDD Polychlorinated Dibenzodioxin
PCDF Polychlorinated Dibenzoflurane
VOD Vacuum oxygen Decarbonization

1 Introduction

Nowadays, it has become apparent that the impact of humans has been detrimental on environment. Since the beginning of the industrial era, the emissions of CO_2 and other green houses gases has continuously increased, resulting in the harmful effects that we all know. For a few years, it has become clear for leaders of most countries that some regulations have to be created to try to limit the damage.

In 2015, most countries accepted to unite to limit climate change, resulting in the Paris Agreement. They stated that their primary objective was to limit the increase of the global average temperature to 1.5 °C compared to the pre-industrial levels [1]. In Europe, the objective to fulfil is carbon neutrality by 2050. According to the European Environment Agency [2], more than 27% of the total estimated green houses gases are produced by the energy supply sector. The sector of the transport represents 23.8% and the industrial sector 20.3%. It is a non negotiable that these three sectors will have to make an effort to successfully respect the 2050 target.

Steel production as an industry has a major impact on worldwide to GHG emissions. In 2020, it contributed to 7% of the global CO_2 emissions [3]. It consists of extremely high energy intensive processes often requiring fossil fuel such as coal or oil. Steel productions route that are less impactful also exist but they still also could be improved.

In this context, the steel production by electric arc furnace, one the least polluting production route, will be analysed in this Master's thesis. A global description of the steel industry will be presented before focusing on this particular route. A research on the possibilities to improve its environmental impact will be realized before attempting to model and compare them. This assessment will consider the emissions and the cost of these alternative pathways.

2 Objective

The objective of this work is to establish a model of the production of stainless steel by electric arc furnace using scrap with some energy transition pathways. For each step of the process, the possibilities of improvement from the current techniques will be compared in terms of environmental impact and cost. All the considered approaches will be represented in what is called a superstructure. The information necessary to build this superstructure is obtain by doing a literature review of the best available techniques of the process, experimental and industrial data.

Once a model of the base case, the most generic traditional case in the industry, is build, alternative pathways are presented for comparison. Ideally, these alternatives are propositions of modification of the base case that would result in a diminution of the CO_2 emissions. They include the fuel switch from natural gas to biomethane or hydrogen for the combustion and the addition of a carbon capture unit. For each configuration, the raw material consumptions as well as the energy requirements will be modelled using "black-box" modelling in order to determine the cost (in €/t steel) and the CO_2 emissions associated (in kg CO_2/t steel). The obtained results will be presented with a sort of sensitivity study conducted by introducing different price scenario for the energy supply of the process as well as their environmental footprint. This can add more value to the analysis, as different hypothesis on the evolution of electricity grid mix, prices or competition in access to renewable fuels in the future are taken into account.

This project could serve as a decision-making tool for the specific electric arc furnace steelmaking industry to estimate which alternatives could be extensively investigated and which ones should not. On a larger scale, the model for this superstructure could also be integrated with other superstructures in what is called a cluster. Connexions between different industries could be created in order to improve the use of product and by-product, excess heat produced by a process or by sharing infrastructures that demand a high investment cost, like a supply network for hydrogen or an on site green electricity production.

3 Literature review

3.1 Steelmaking industry : generalities

Steel is one of the most important materials in the world. Different grades exist depending on the composition. Carbon steel is the most simple of them but alloying metals such as chromium can be added to improve corrosion resistance. It has many applications in plenty of sectors from buildings and infrastructures to transport, electrical equipment or domestic appliances [4]. Its production has been stable for the last few years, reaching 1 885 million tons in 2024 [5] The biggest steel producer is China which is responsible of more than half of the world production.

Even if the majority of steel is still produced using the conventional method based on the blast furnace and basic oxygen furnace (BF-BOF), the electric arc furnace (EAF) accounted for 29.1 % of the world steel production in 2023 [4]. In 2006, steel production by electric arc furnace or direct reduced iron (DRI) represented 40.2% while blast furnace and basic oxygen furnace represented 59.8% in Europe [6]. Figure 1 presents the four steel production routes currently implemented worldwide. First is the blast furnace and basic oxygen furnace route, which is still the most frequently encountered technology. Next are the smelting and direct reduction and finally, the scrap-based EAF, also known as secondary steelmaking.

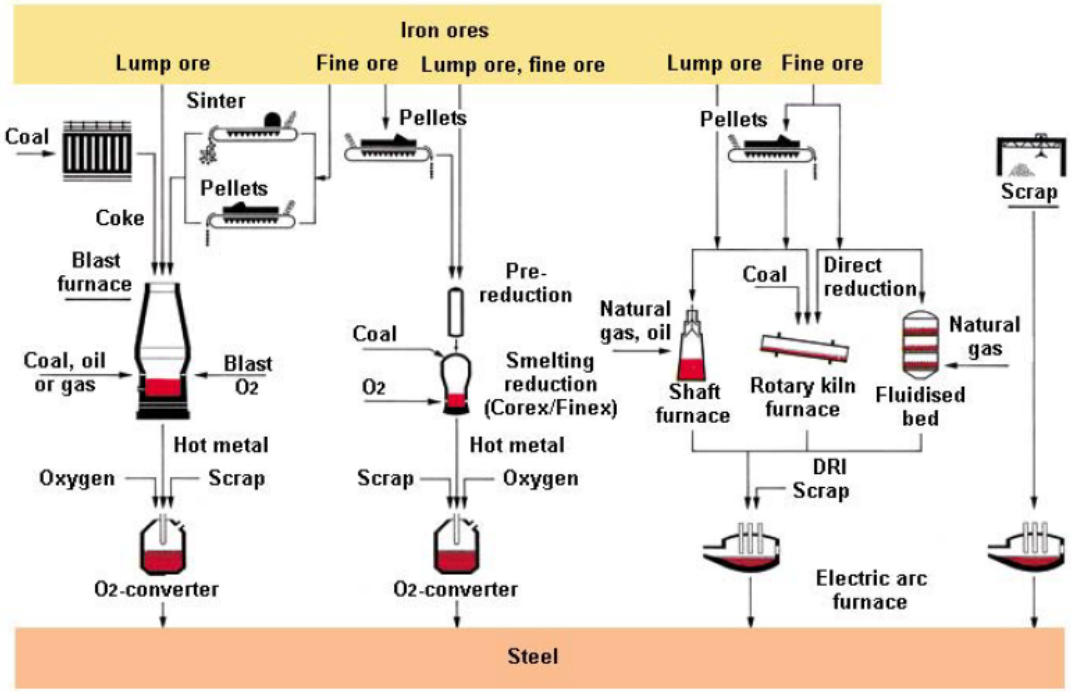

Figure 1: Different routes for steel production worldwide [6]

As it is the main interest of this study, the secondary steelmaking route will be described in-depth in a dedicated section (see section 3.2). A brief description of the other production

routes is presented in sections 3.1.1-3.1.3.

3.1.1 Blast furnace and basic oxygen furnace route

As a preparation step for the blast furnace and the reduction methods, iron ore is turned into pellets or sinter. Coke is prepared by dry distillation in a coke oven [6]. In the blast furnace, the pellets and sinter are reduced into liquid iron also called "hot metal". Coke and coal are used as fuel into the furnace, providing the energy required for melting. In the furnace, they also react with the oxygen that is injected and form carbon monoxide which is the actual reducing agent of the metal.
In addition to these materials, some fluxes, such as lime or dolomite, are fed. They will help to separate the impurities and unwanted parts of the ore, the gangue, from the melted metal. A by-product called slag is formed and collected with the hot metal.
During the following step, the hot metal is sent to the basic oxygen furnace. Its objective is to decrease its carbon content and obtain the desired product, steel.

The main source of energy for this steel production technology is usually coal and other liquid or gas fossil fuels. As a result, this production route is responsible for high emissions of CO, CO_2, dust and other air pollutants [6].

3.1.2 Smelting route

Unlike the blast furnace operation, the smelting is a process where iron ore gets reduced without using coke, which is replaced by coal. Without needing coke oven, the process is also less selective in the quality of coal permitted. The two main commercialized processes of smelting are COREX and FIREX. Figure 2 shows a comparison of both.

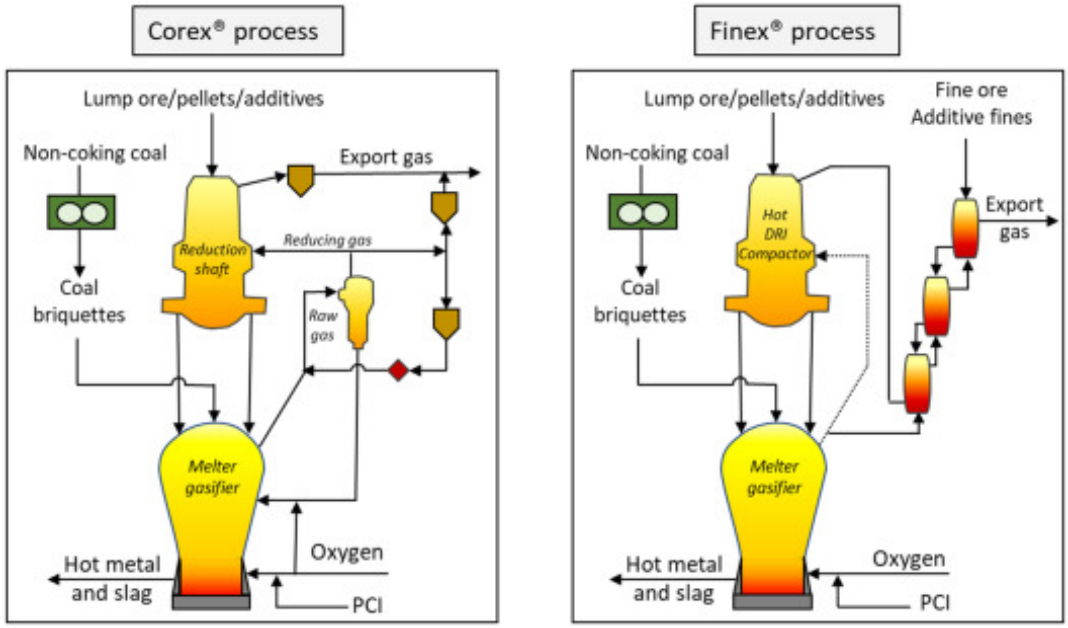

Figure 2: COREX and FIREX processes for smelting reduction [7]

The COREX (coal reduction) smelting operates in two stages, the reduction shaft and the melter gasifier [7]. During this last step, the oxygen and the coal introduced will produce a gas composed of CO and H_2 that that will be injected with the ore as the reducing agent in the first step. After that pre-reduction, the liquid metal along with some slag is obtained at the exit of the melting vessel. The energy necessary for the smelting is provided by the combustion of coal [8]. To obtain steel, the hot metal has to be fed to the BOF, similarly to the product of the blast furnace. The Finex process is very similar, except that the reducing shaft is replaced by a fluidized bed [7].

3.1.3 DRI route

Direct reduction is able to process iron ores and produce a material called direct reduced iron (DRI) that can be used as raw material for the EAF. Different methods of iron reduction are possible based on the chosen reducing agent: natural gas, coal or hydrogen. The latter is the best in terms of emissions because it produces water instead of CO_2 [6]. To be easily transported, the reduced iron can be made into pellets, called hot briquetted iron (HBI). This way, it can be transferred to an EAF that is located away from the ore-reduction plant [9].

3.2 Description of the electric arc furnace steelmaking

Compared to the previously mentioned steelmaking routes, the secondary steelmaking route enables the reduction of the impact of the steel production. It requires less fossil energy and uses recycled steel as a main raw material, in a circular economy approach.

The process to produce stainless steel from scraps consists of three major steps: the primary metallurgy where the scrap is melted in the EAF, the secondary metallurgy where

the molten metal is treated in a vacuum oxygen decarbonizer (VOD) or an argon oxygen decarbonizer (AOD) in order to reach the targeted composition for the stainless steel and, finally, the casting and the rolling to obtain a product of the desired shape [6]. A schematic description of the whole process is presented in Figure 3.

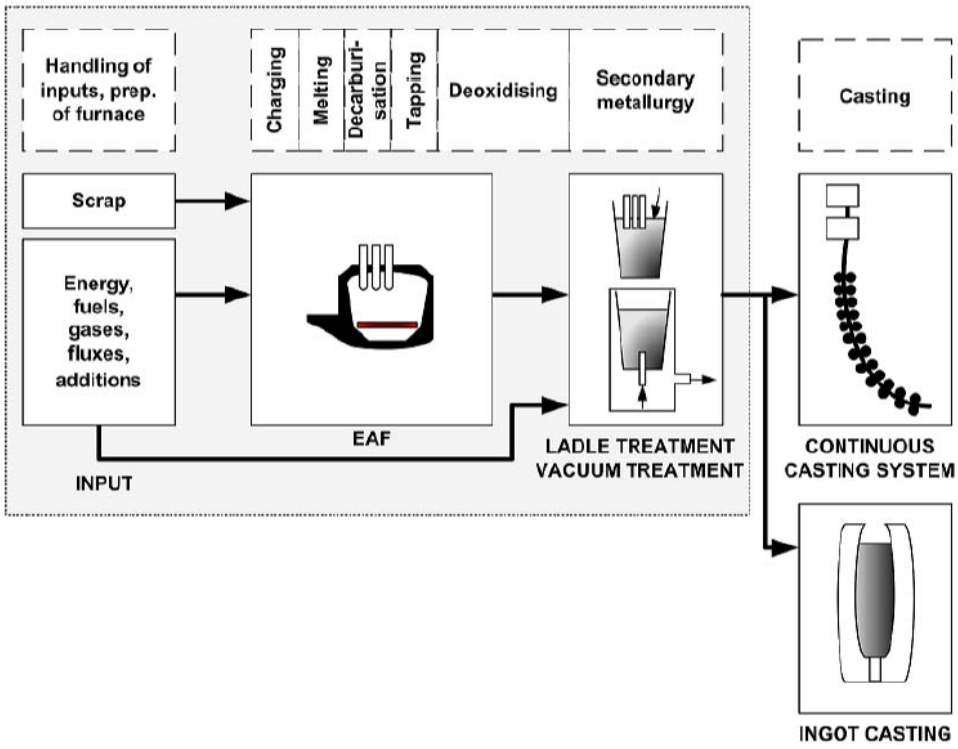

Figure 3: EAF steel production route [6]

3.2.1 Electric arc furnace

The EAF is a big vessel covered on the inside by refractory material, made mostly of MgO to mitigate heat losses [10]. Graphites electrodes are placed on the top of the furnace, which can be opened for the charging. Because of this, an uncontrolled amount of air can penetrate and participate as a reactant, in particular the oxygen. It does not represent a problem at the stage, it will just increase the off-gas volume and by diluting it. The EAF is also equipped with oxygen injectors and off-gases evacuation. Doors are also located on the side for the tapping, the collecting of the products [11]. This can be seen in Figure 4.

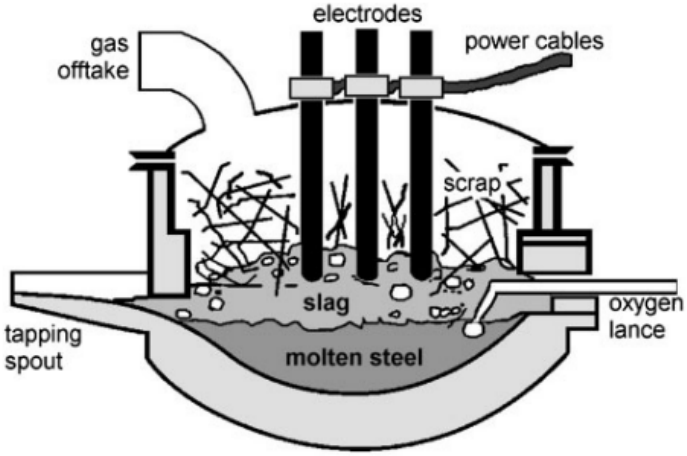

Figure 4: Representation of the electric arc furnace [12]

The EAF operation consists of four phases: the charging, the melting, the flat bath (or decarburisation) and the tapping [13]. Thus, the furnace works in a discontinuous way, comparable to a batch reactor. The duration of one melting cycle is approximatively 1 hour [14] and the temperature inside the furnace can reach up to 1600°C [15]. A detailed description of each phase is provided below.

First, scrap is charged in the furnace with additional alloy metals, such as ferro-chromium or ferro-silicon to tune the composition of the steel [12]. In addition to the metals, some mineral materials, called fluxes, are introduced in the EAF. These include usually lime and dolomite [6]. Their role is to trap the metallic oxides inside the by-product called slag [16].

The charging is often carried out in two or three steps, with an intermediate melting phase to ensure a homogeneous melting of the cold scrap [10]. During melting, oxygen is injected to oxidize some unwanted elements present in the scrap. These can be pollutants, such as hydrocarbons and sulphur, or metals whose concentration has to be lowered to meet the requirements for the desired grades of steel. These metallic and non-metallic oxides will end up in the flue gas, as CO and CO_2, or will be captured by the fluxes to form the slag, a liquid by-product of the furnace that sits on top of the molten metal. Depending on the initial composition of the scrap, different oxidation reactions are possible inside the melt. A list is presented from Equation 1 to 10 [17].

$$Si + O_2 \longrightarrow SiO2 \ \Delta H = -8.94\text{kWh/kg Si} \tag{1}$$

$$Mn + 0.5O_2 \longrightarrow MnO \ \Delta H = -1.93\text{kWh/kg Mn} \tag{2}$$

$$2Cr + 1.5O_2 \longrightarrow Cr2O_3 \ \Delta H = 3.05\text{kWh/kg Cr} \tag{3}$$

$$2Fe + 1.5O_2 \longrightarrow Fe_2O_3 \ \Delta H = -2.05\text{kWh/kg Fe} \tag{4}$$

$$Fe + 1.5O_2 \longrightarrow FeO \ \Delta H = -1.32\text{kWh/kg Fe} \tag{5}$$

$$C + O_2 \longrightarrow CO_2 \ \Delta H = -9.10\text{kWh/kg C} \tag{6}$$

$$2Al + 1.5O_2 \longrightarrow Al_2O_3 \ \Delta H = -5.29\text{kWh/kg Al} \tag{7}$$

$$Mo + O_2 \longrightarrow MoO_2 \ \Delta H = -1.70\text{kWh/kg Mo} \quad (8)$$

$$S + O_2 \longrightarrow SO_2 \ \Delta H = -2.75\text{kWh/kg S} \quad (9)$$

$$2P + 2.5O_2 \longrightarrow P2O_5 \ \Delta H = -5.54\text{kWh/kg P} \quad (10)$$

Once all the raw materials have been introduced into the furnace, the phase of the flat bath will start. This means that everything will be kept inside the furnace for 50 min [14]. The goal is to allow every product to correctly form and all the gases to leave the furnace.

Finally, the tapping stage consists of collecting the slag and the molten metal separately. This is done by tilting the furnace, on one side to collect the slag and on the other to collect the melted metal, as it can be seen in Figure 5. After that, the EAF is ready to start a new cycle [6].

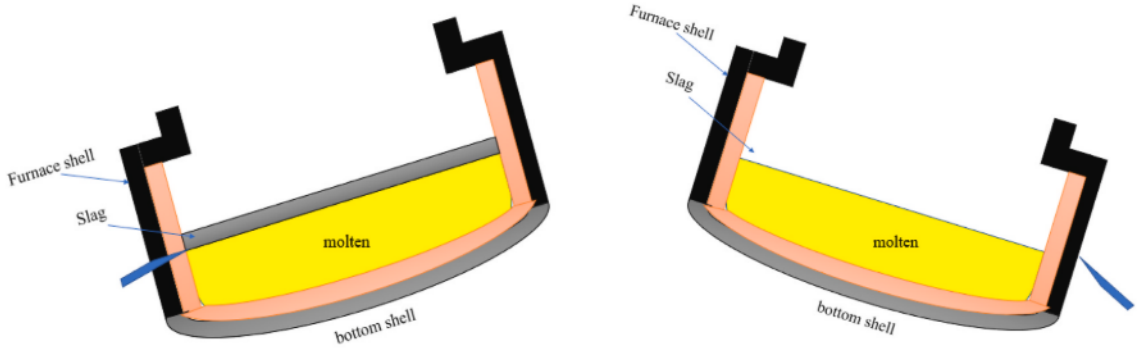

Figure 5: Drawing representation of the tapping by tilting [11]

The main source of energy for the melting is the electricity provided by the electrodes, specifically the electric arcs that they produce. A supplementary source of energy can be added via fossil fuels inside the furnace to ensure the homogeneity of the melting. Currently, the best technique is to provide heat through oxy-combustion during the melting phase [6].

In the case of low-alloyed steel production, carbon powder and oxygen can be injected together in the EAF. Their reaction will form carbon monoxide that will create a foamy slag. This practice is really common since it offers several benefits. It creates a barrier that helps to limit the consumption of electrodes and refractory materials. It also helps to enhance thermal homogeneity inside the furnace [6]. The condition for good foaming is to have an adequate viscosity that depends on the iron oxide content of the slag. However, for steel that contains a higher concentration in chromium, this practice is not so efficient. The chromium present in the steel will have a higher tendency to react with the oxygen than the iron, resulting in a viscosity that is not suitable for the foaming. This also causes a loss of chromium which is counter-productive. This technique is thus not recommended for the production of stainless steel [18].

3.2.2 Secondary metallurgy

The second step of the process is the decarburization of the steel. To be defined as stainless steel, chromium content has to be relatively high, between 24 and 26% for the 314 grade stainless steel [19]. Carbon content, however, is kept very low for a good quality stainless steel [20], [21], around 0.2% for the same 314 grade steel [19]. In order to remove the excess carbon while maintaining sufficient levels of chromium, two types of convertors are possible: Argon Oxygen Decarbonization (AOD) or a Vacuum Oxygen Decarbonization (VOD) converter. They are illustrated in Figures 6 and 7.

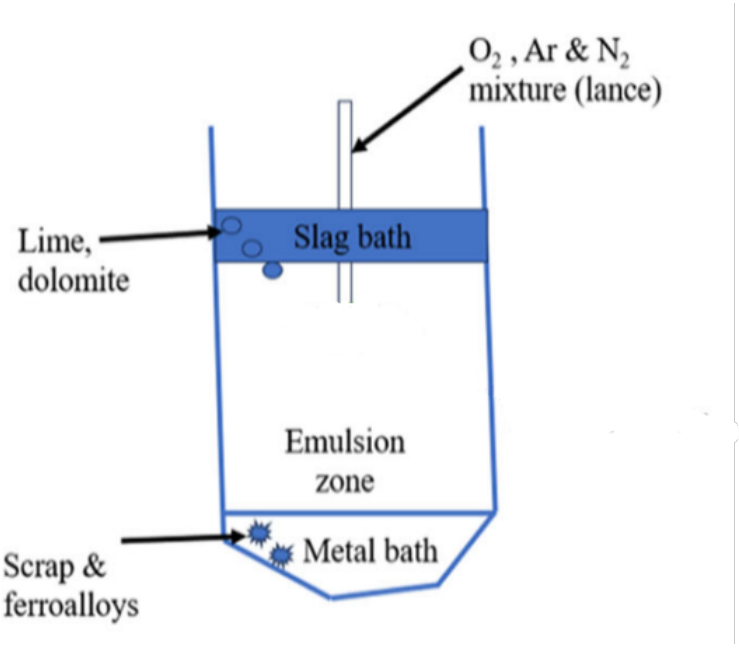

Figure 6: Representation of an AOD converter, modified from [22]

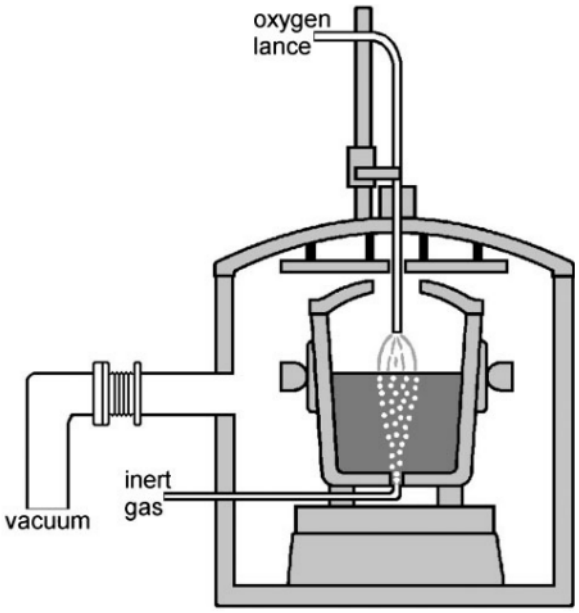

Figure 7: Representation of a VOD converter [21]

In both cases, the molten metal is introduced into the vessel with some fluxes and alloy metals. This will help to reach the required final composition and capture some impurities still present in the steel. Oxygen is injected in the vessel along with inert gases, N_2 and Ar to reduce the vapor pressure of the CO_2 produced inside the converter by dilution.

The need to reduce the vapor pressure of CO_2 inside the vessel can be explained using Figure 8. This is a Ellingham diagram that shows the variation of the Gibbs free energy change for the oxidation reactions are as a function of temperature. The lower the curve is, the more thermodynamically stable is the oxide. The darker region of the graph represents the temperature range for steelmaking, around 1600°C. Initially, the oxidation of the carbon is the reaction that is favoured but as more carbon reacts, its activity decreases and the oxidation reaction of the chromium becomes the favoured one. In order to shift this equilibrium, the partial pressure of CO_2 has to be lowered. No external supply of heat is needed for this process step, since the heat of the product that is coming out of the EAF is sufficient for the conduct of the process in this vessel.

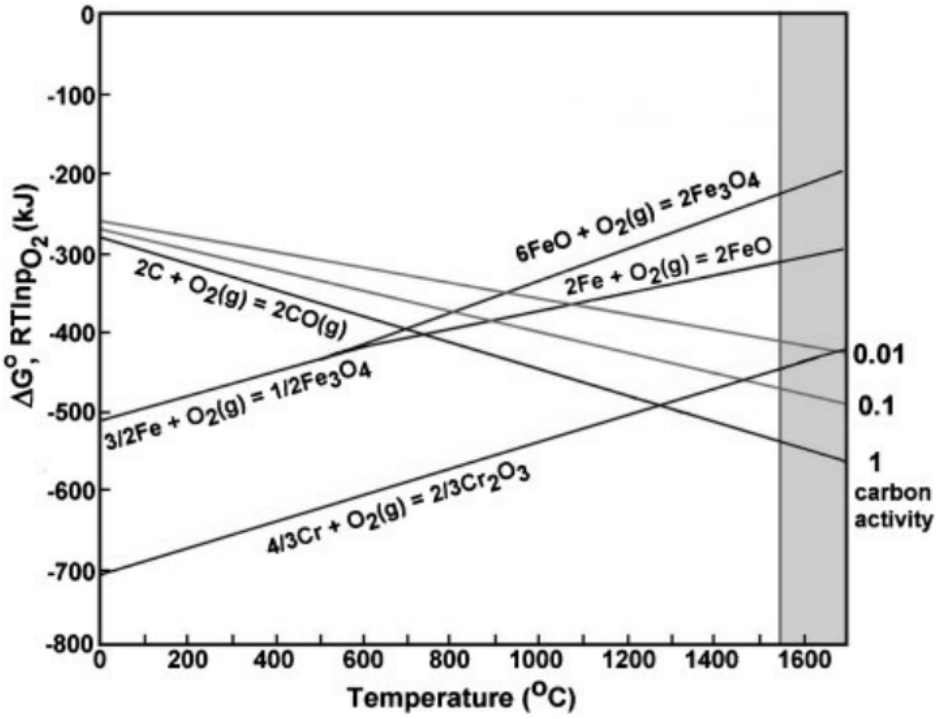

Figure 8: Oxidation reactions in the AOD and VOD converters [21]

The two converters are using two different methods to decrease the partial pressure of CO_2. For the AOD, the injection of inert gas, a mix of argon (Ar) and nitrogen (N_2), in different proportions is used to avoid the loss of chromium. Nitrogen is usually favoured due to its lower cost. However, using too much nitrogen is not possible because this could result in nitrogen insertion in the steel, lowering its quality [23]. While a small amount of inert gas is also introduced in the VOD, a vacuum pump is added to the system to reduce the pressure inside the vessel, subsequently leading to the CO_2 pressure reduction.

At the end of the treatment, some off gas consisting of CO_2, N_2, Ar and the unreacted O_2 is released. A slag is also produced and collected before obtaining the desired product, the stainless steel [24].

Most of the time, both techniques are suitable as secondary metallurgy treatment. The decision is made based on the cost or the product that is needed, because the vacuum pump is usually more expensive to operate but VOD is better very low carbon is needed [23].

3.2.3 Casting and rolling

After refining, the molten stainless steel is transferred to continuous casting, which converts the liquid metal into semi-finished products such as slabs. Figure 9 shows an illustration of this step. At this stage, the liquid steel is poured into a water-cooled mould where the steel solidified progressively [6]. The long strand is then cut to the required slab length.

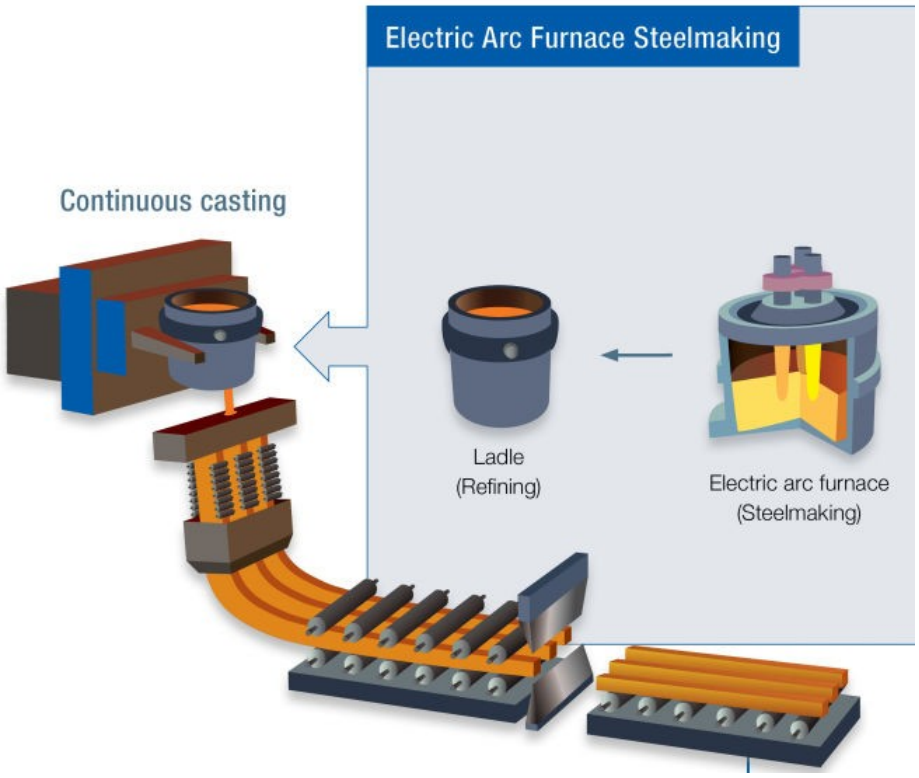

Figure 9: Description of the casting step [25]

Once the slabs are produced, they are reheated in a furnace before entering the hot rolling mill, which is depicted in Figure 10. Hot rolling has to be carried out at high temperature, slightly below than the fusion temperature, so that the steel remains ductile and can be deformed more easily [26]. The slab passes through a series of rolling stands that gradually reduce its thickness and change its shape depending on the final product.

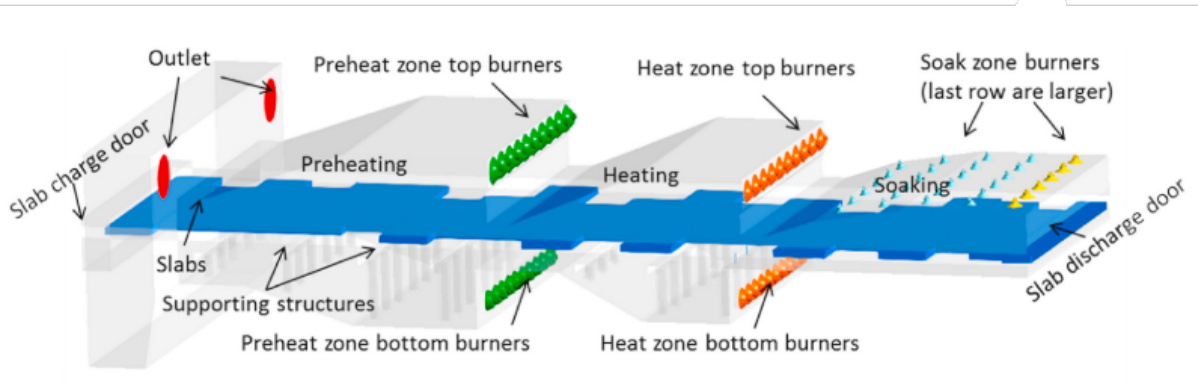

Figure 10: Illustration for the heating of the steel [27]

From all the steps involved in the EAF-based steel production, rolling is the most energy-intensive step. The heating furnaces are powered by natural gas and work continuously to

ensure an homogeneous temperature of the steel. This is important to avoid the appearance of local defects inside the material that could lower its mechanical properties [6].

3.3 Treatment and reuse of the by products

There are four major type of wastes in the process, namely the slag, the refractory material, the off gas and the dust. A way to limit their impact is to find ways to reuse or recycle these by-products. Some are very common and used almost directly, while some new methods are studied in order to further improve the reuse of these by-products.

3.3.1 Treatment and use of the off-gas

As they exit the electric arc furnace, fumes are collected with the help of a hood placed above the furnace [6]. These fumes contain different sorts of pollutants ranging from CO and CO_2, to SOx and NOx, heavy metals and organics, in particular PCDD/F (Polychlorinated dibenzodioxins and Polychlorinated dibenzofurans). Bag filters are used as the first treatment. In rare cases, electrostatic precipitators or wet scrubbers are used [6]. In the case of carbon steel, the off gas can contain a non negligible fraction of CO that was introduced to form the foamy slag. A post combustion chamber is added where that CO reacts with oxygen to form CO_2 [6].

For the SOx and NOx, they are collected in the same bag filter than dust [6]. Regarding the PCDD/F, these toxic molecules can be produced inside the EAF off-gas under very specific conditions. Precursors, that are organic particles sometimes present in the scrap, will react at temperature between 600 and 800°C to form the PCDD/F following the so-called novo reactions. A way to avoid these reactions is to heat the gas between 800 and 1000°C to break all the PCDD/F and rapidly quench to 200°C to avoid their reformation [6].

The temperature of the gas can reach between 1200 and 1750°C [13] at the exit of the EAF. A high amount of energy could be recovered from these fumes and be reused directly in the process or to produce steam or electricity. A process called CONSTEEL uses the heat of the off gas to preheat the steel scrap that will enter the EAF in a counter current flow [6]. As a consequence, a reduction of time residency of 10 minutes can be observed. However, this system can also have some downsides. If the scrap contains hydrocarbons, the pre-heating will release VOC that require a more complicated post combustion treatment The formation of plug at the entrance of the furnace is also possible when the pre-heating is too intense and melts some scrap.

A few other methods of waste heat recovery have been investigated. A study by Steinparzer et al. [28] tested a pilot to produce steam using an evaporative cooling system. They proposed to replace the cooling step, traditionally performed with cooling water, by a heat exchanger using molten salt as heat transfer fluid. The aim of this study was to analyse the corrosion and erosion of the material inside of the heat exchanger, from the side of the molten salt caused by the chlorine and from the side of the EAF gases. The high dust content can lead to high material stress. The intermittency of the process is also problematic.

A solution to some of these issues is to operate a totally different way of heat recovery. In their work, Hartfuß et al. [29] studied a novel waste heat recovery technique. Their proposition is to use an element that has a higher heat storage density than steam. Calcium hydroxide is the material studied in this case. At high temperature, $Ca(OH)_2$ gets dehydrated following the reaction presented in Equation 11. At lower temperature, the reaction is reversed and the heat is released.

$$Ca(OH)_2 \rightleftharpoons CaO + H_2O \; ; \; \Delta H_R = 104 \text{ kJ/ mol} \tag{11}$$

In terms of chemical equilibrium, the dehydration reaction needs high temperature steam, above 519°C. As the measured temperature of the EAF off-gas is around 600°C, the dehydration is possible and the $Ca(OH)_2$ is, thus, assumed to be a good alternative material for heat recovery. In practice, calcium hydroxide particles are injected into an entrained flow reactor with the off-gas exiting the post-combustion chamber. Hot lime particles are collected after passing through a cyclone separator. They are introduced into a bubbling bed reactor where the hydration reaction occurs and steam is formed to produce electricity. One drawback that has been identified is that the heat storage material could deteriorate in contact with the dust present in the off-gas. The solution is to directly use the contaminated lime as fluxed raw material for the EAF, according to the principle of circular economy.

3.3.2 Treatment and use of the slag

The slag collected at the exit of the EAF (EAFS) is a liquid phase containing the mineral lime and dolomite and the metal oxides alongside some impurities that have been trapped. Once it solidifies, it has the appearance of a rock and can have a multitude of uses. Currently, it is mostly landfilled [30] or used in the preparation of cement and other construction materials [6], but some studies have been accomplished to find ways to implement a safe reuse and recycling of this multi-purpose matter. A non exhaustive list of applications from the literature, from the most classic to the most innovative is presented in this section.

The article from Rudnik et al. [30] presents various studies that have been conducted to improve the valorisation of the EAFS by recovering metals by hydrometallurgy. The composition of the slag is very complex with a wide variety of elements present in different mineral phases. The studies focus on the recovery of Fe, Cr, Ca, V, Mn, Ti, Mb and Nb. The efficiency of recovery is improved by perfecting the leaching conditions or by adding diverse pr- treatment such as grinding and roasting, micro-wave treatments, or pyrometallurgical reduction. The use of bio-leaching techniques is also discussed. In this case, microbial cultures of bacteria and fungi are used for their capacity to produce acid instead of conventional HCl or H_2SO_4. Extraction efficiencies were found encouraging for Mg and Zn (75 and 60%) but did not exceed 30% for other metals.

A study by Godson et al. [31] proposed to use EAF slag as a replacement for granite for sub-layer ballast of railway. They compared both products by evaluating their chemical and physical properties, subjecting them to some stresses comparable to real conditions

of rail track. They also evaluated the safety of using slag by analysing its environmental performance. According to their tests, EAF slag is a suitable material for ballast. It was found to have a better resistance to abrasion and impact, a better strength and a better resistance to deformation under load. In cyclic tests, EAF slag was better than granite. In terms of toxicity, they measured the concentration of heavy metals in a sample obtained after leaching of the slag. The results of the concentration measurements show values that are lower than the "hazardous waste limit" presented in the article.

In the study of Kanon et al. [32], the slag is presented as a reinforcement material for glass fiber-epoxy composites that could serve as an alternative to lead in X-ray shielding equipment. This replacement would offer a non-toxic solution that could also better fit applications where flexibility is required. Composite materials seem to be adequate for this since they are composed of polymer matrix while some specifically showed X-ray attenuation properties which can even be increased by adding waste fillers such as eggshell, bone waste and crab shell. This particular study tested the mechanical performance, thermal stability and X-ray absorption of EAFS in composite materials. The results showed that the addition of slag particles will decrease the tensile strengths and flexural strengths but increase the heat isolation. Concerning the X-ray protection, the slag particles were beneficial as the maximum value was recorded for a 30% concentration in weight.

Other sustainable uses of slag include its combination with synthetic fertilizer to improve soil quality and bring nutrients to plants [33], the replacement of lime for the treatment of acidic waste water [34] and CO_2 sequestration by forming calcium or magnesium carbonates [35].

3.3.3 Treatment and use of the dust

Initially, the dust collected from the EAF is considered a hazardous waste because of its heavy metals and PCDD/F content [36]. The conventional way to recycle them is to use them in the preparation of concrete, asphalt [37] or even in mortar [38]. However, techniques have been studied to extract some metals of interest and use them in more valuable applications. The most used currently is the Waelz process. The dusts are processed through a rotary kiln to remove the unwanted components [39]. In the end, a mixture of zinc oxide and lead oxides called Waelz oxide is obtained. The high zinc content of EAF dust (around 25% in mass of the composition [39]) makes it a very interesting zinc source.

The Waelz rotary kiln process is an efficient way to recover zinc oxide from the EAF dust [36]. Unfortunately, this process is also a source of PCDD/F emissions. Rapid heating and quenching can also be a solution but some alternative methods have also been tested to mitigate these emissions. Li et al. [36] have studied the efficiency of the injection of powder-activated carbon (PAC) and a biosolution named NOE-7F to remove PCDD/F from the off gas of the Waelz process. They based their works on other articles that already tested PAC for this application but it was found to only have an adsorption effect, not a degradation effect. The goal of this new biosolution is to directly target the precursors of the PCCD/F. This NOE-7C solution is an organic enzyme made with rice wine, molasses,

acetic acid and bacteria. Their results showed that PAC was effective to remove PCCD/F but a distinction has to be made between them. The lower chlorinated ones were better removed than the higher chlorinated ones. In the case of a low mass of PAC injected, they observed that it played no more its role of removing agent but acted as a precursor of PCCD/F, resulting in a higher pollutant concentration than before. For the bio-enzyme, it was observed that it had an effect on the higher chlorinated substances. The use of PAC and NOE-7F together could be possible to combine the strength of the two products.

In the study by Kamali et al. [37], a hydrometallurgy process consisting of two leaching steps and a co-precipitation has been studied to form a magnetic $MgFe_2O_4 - CaFe_2O_4$ powder. This powder was tested as a photocatalyst for the degradation of methylene blue dye. In their study, they first optimized the catalyst synthesis by determining the optimal temperature and acid concentration for the best metals recovery. They used a few characterisation methods, in particular XRD and XPS, to prove that they correctly formed the expected molecules. Finally, they showed that their sample was able to degrade the dye with a 45% efficiency under visible light radiation.

Other applications for the zinc oxide obtained from EAF dust (EAFD) can be found. For example, the study of Liptai et al. [40] tested the preparation and effectiveness of varistors, which are protection devices for electrical network in the case of lighting or over-voltage. After treating the dust by alkaline leaching and calcination, they obtained a powder that was composed at 79% in mass of zinc, very close to the 80.35 % theoretical value for pure ZnO. They finally formed tablets to be sintered before testing their electrical properties. They concluded that their samples worked in the same way than traditional zinc oxide, which is promising for the recycling of EAF dust.

3.3.4 Recycling of the refractory material

The refractory lining of the electric arc furnace can wear through time. The use of foaming slag can help to prolong their lifetime but they ultimately have to be replaced after around 480 cycles [41]. Most of the time, they were not used but an application has been tested for a direct application in the EAF. As the composition of refractory is mostly MgO, it is similar to what is used as fluxes materials. A study by Conejo et al. [41] studied the addition of this spent refractory in an electric arc furnace using a mix of scrap and DRI. They noticed that this reuse had a few advantages. It allowed an economy in fluxes materials, a lower electrical energy consumption, a shorter melting time and even an elongated lifetime for the refractory.

3.4 Alternative pathways

CO_2 is the pollutant that is the most emitted by the EAF steelmaking route. In each step, direct emissions are observed : from the oxidation of the carbon in the metal and the electrodes or from the combustion of fuel. Additional emissions also arise from the production of electricity, fuel and raw materials. Even though nothing can be done for the latter expect using electricity produced from renewables, direct emissions of the steel production process

could be improved using different methods.

The electric arc furnace route is already an improvement from the traditional BF-BOF route, implementing a blast furnace that uses coke as reducing agent for the iron. Average CO_2 emissions to produce 1 ton of crude steel are 2.32 ton for the BF-BOF and 0.7 ton for EAF[42]. However, in order to achieve the objectives of low carbon steel production, some improvement can still be done to further decrease the emissions of the EAF steel production and the global steel production industry.

3.4.1 DRI

As it is relying on natural iron ores, DRI has a higher proportion of gangue, undesired minerals, than recycled steel scrap. Its composition can also vary based on the quality of ores or the chosen process. From the relatively low proportion of EAF in the world steel production, it is supposed that scrap availability is currently sufficient for the existing EAF plant. However, there is a high probability that the relative share of EAF-based production will increase in the future. Hence, the need for scrap will likely increase, making it harder to provide the necessary amount for steel production. Following this conclusion, an investigation to find a new, virgin material has been started, resulting in the focus on direct reduction. In current EAFs that use DRI, the material is most of the time mixed with scrap to ensure a good running of the process [13].

As the ratio of DRI versus scrap increases, some operating parameters have to be modified [43]. Due to the amount of impurities contained in DRI, a larger mass of metal is needed to make the same amount of steel. The amount of ferro-alloys also has to be increased because the virgin material contains mainly iron which is not sufficient to make steel. More fluxes are also necessary to capture the excess of impurities. As the total input mass is greater than in the 100% scrap case, the energy needed to melt everything also needs to be increased. Few data are available to describe the behaviour of these parameters based on the proportion of DRI in the input mix. Some studies tried to build models predicting the values of the parameters [44] [45]. However, the variability of the composition and the quality of iron ores makes it harder to find a model that is robust and reliable for every situation.

3.4.2 Fuel switching

Another alternative to decrease the emissions of the process is to substitute the fossil fuel used in the different steps of the process. In the EAF, the improvement will be limited as the proportion of natural gas used is minor. The CO_2 formed during the degradation of the electrode cannot be avoided. For the hot rolling step, however, fuel switching will have a higher impact as this step is the one that requires the most fossil fuel energy.

3.4.2.1 Biomethane

Biomethane is a purified biogas produced by digestion of biomass matter [46]. Compared to the fossil fuel, it is identified as a carbon neutral fuel. Its biogenic CO_2 emissions are considered to be compensated by the ones absorbed by the biological source material. The purification will ensure that CO_2 is removed and only the valuable energy-dense molecule is kept. This way, biomethane's composition and calorific value are the most similar the one of natural gas. This make its use as a sustainable replacement for natural gas easier to set up. The same burner can be used a mix of both natural gas and biomethane is possible to facilitate the transition **<empty citation>**

A few recent projects have investigating the use of biomethane or syngas in the EAF steel production route. Ternium, a South American steel producing company started to replace a part of their natural gas by biomethane in their plant in Brazil in 2020 [47]. They make steel by following the conventional BF-BOF route but it shows that biomethane is adapted to the steelmaking industry. By only replacing 34% of their natural gas consumption, they expect to reduce their green house gas production by the same amount.

In their studies, Xue et al. [48] investigated the switch to biomethane combustion as the additional heating inside the EAF. Based on their calculation, this could help to reduce by 8.9 kg their CO_2 production by ton steel which is equivalent to 2.2% of their total emissions.
Guo et al. recently modelled the use of syngas in combination of natural gas for the heating furnace of the rolling [26]. Their objective was to determine the optimum mixing proportions to ensure the highest heating efficiency while also improving the CO_2 emissions all at reasonable cost.

3.4.2.2 Hydrogen

Hydrogen is an high energy intensive molecule that could also be considered for industrial fuel switching. Its main advantage is that no CO_2 is directly produced during its combustion, avoiding the need for post-combustion fume treatment. Depending on its method of production, a different colour is associated to the molecule that will symbolize its impact [49]. The best is the green hydrogen, produced by electricity generated from renewable energy. The most common is grey hydrogen, produced by steam methane reforming but the addition of a carbon capture and storage process (blue hydrogen) allows to decrease its high environmental impact. A major drawback of H_2 is that its volumic energy density is lower than natural gas [50], necessitating a higher fuel volume to produce the same amount of heat.

Some industrial projects or studies exists on the use of hydrogen in the electric arc furnace steelmaking. Sarted in 2022, an European project called DevH2forEAF,reuniting Italian and Spanish electric arc furnace steelmaking plants, has investigated the use of hydrogen inside the EAF. Its main objectives were to design burners that could work with a mix of natural gas and hydrogen or with 100% H_2, to evaluate the performance and the steel quality while also analysing the risk to come up with safe procedures.

In their article, Della Rocca et al. [51] present a 100% hydrogen flameless Smart burner produced by Tenova, in Italy. It has been specially design to be used in the rolling process. Their test using a mixture of natural gas and pure hydrogen showed good results in the production of NOx compared to traditional burner using the same fuels.

In 2023, Ovako was the first steel producing company in the world to start to produce green hydrogen on a steelwork [52]. By feeding it into the heating furnace before the rolling, they are able to almost reduce completely the emissions of this step of the process. Located in Sweden, it is also the biggest electrolysis plant in the country.

3.4.3 Carbon capture

Another technology that could be implemented to bring process emissions down is the carbon capture treatment of the flue gas.

3.4.3.1 Chemical absorption

Chemical absorption with amine solvents is the most mature and widely deployed technology for CO_2 capture with monoethanolamine (MEA) being the most studied amine. The main reaction of carbamate formation can be written as the Equation 12 [53].

$$CO_2 + 2RNH_2 \rightleftharpoons RNHCOO^- + RNH_3^+ \tag{12}$$

The process operates across two main columns: an absorber, where the flue gas contacts the amine solution counter-currently and a regenerator (desorption), where the rich amine solution is heated to release CO_2 and regenerate the lean solvent. A exchanger between the two amine streams enables significant energy recovery inside the process [54].

When investigating the compatibility of the EAF with such carbon capture, the discontinuity of the steelmaking process makes it hard to correctly size and design the unit.

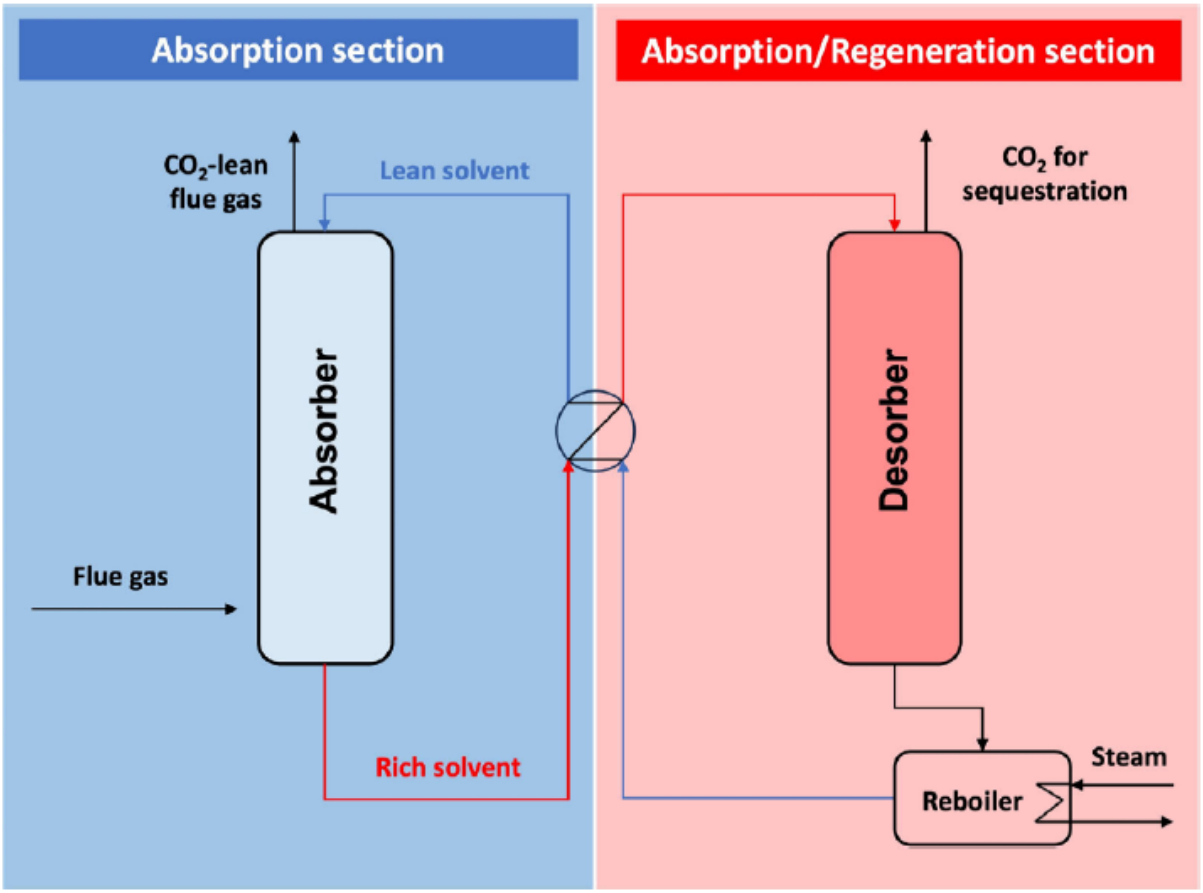

Figure 11: Representation of chemical absorption [54]

3.4.3.2 Calcium looping

Calcium looping (CaL) is a CO_2 capture process based on the reversible reaction between carbon dioxide and calcium oxide expressed in Equation 13 [55].

$$CaO + CO_2 \rightleftharpoons CaCO_3 \tag{13}$$

Carbonation takes place in a circulating fluidised bed reactor at 600–700°C. The $CaCO_3$ formed is then transferred to a second reactor (calciner), where it is heated to 850–950°C to regenerate CaO and release a concentrated CO_2 stream (>85 vol%) [55]. This process is termed a loop because the CaO sorbent circulates continuously between the two reactors [55]. The main advantage of the calcium looping process in the steel industry is that lime is a very low cost material that is already used as a raw material in the process. Also, the heat available from the calcination reaction can be valorised for steam-cycle electricity generation, significantly reducing the net energy penalty of the process.

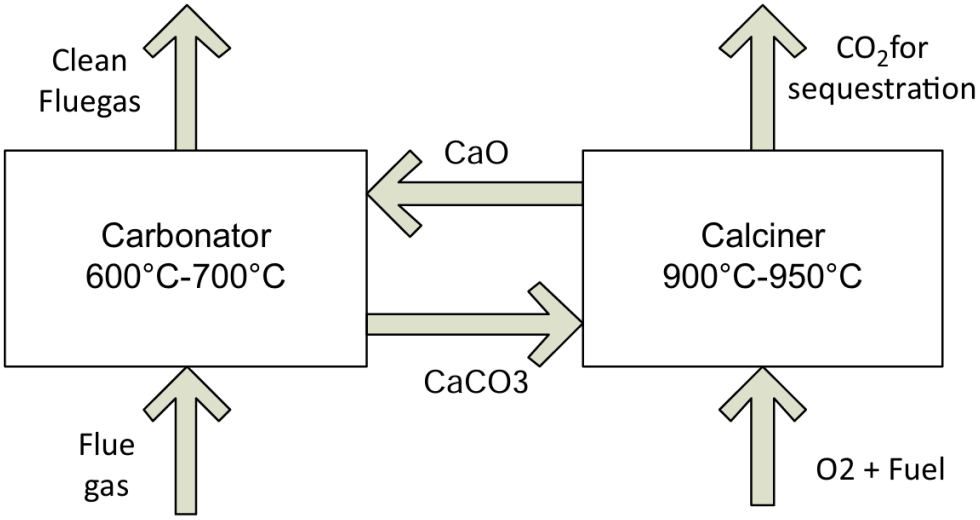

Figure 12: Representation of calcium looping [55]

3.4.3.3 Pressure swing and temperature swing adsorption

Pressure Swing Adsorption (PSA) and Temperature Swing Adsorption based on the capacity of certain porous solid materials to selectively adsorb CO_2 at high pressure and desorb it at low pressure or under vacuum [56]. The basic cycle comprises at least four steps: pressurisation, adsorption, depressurisation and regeneration. The most commonly employed adsorbent materials are zeolites, activated carbons, and MOFs (Metal-Organic Frameworks).

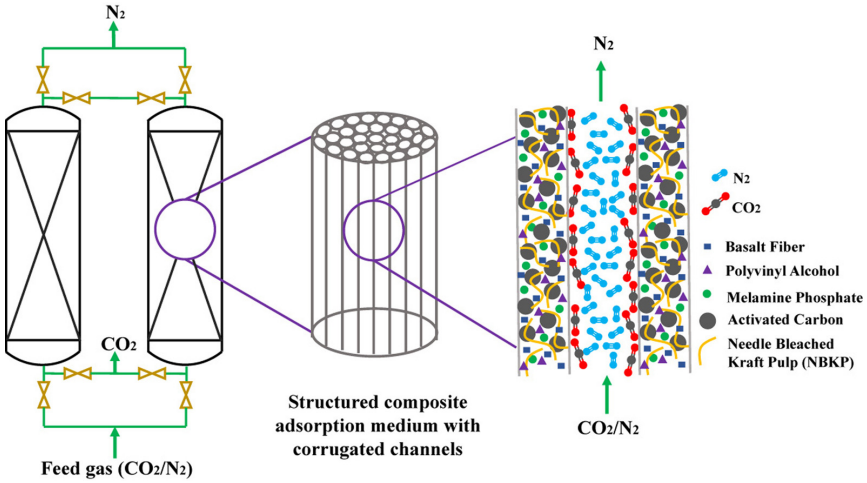

Figure 13: Representation of adsorption [56]

3.4.3.4 Membrane

Membrane separation is based on the differences in the permeability of gas mixture components through a selective material. For CO_2 capture, three main families of membranes are being investigated. Polymeric membranes remain the most industrially developed [54].

Membranes based on polyimide, polymethacrylate, and silicone (PDMS) are used in commercial applications. Inorganic membranes (ceramic, zeolitic, MOF-based) offer better thermal and chemical stability, but their large-scale fabrication remains costly [54]. Mixed matrix membranes (MMMs) combine inorganic fillers (MOFs, zeolites) within a polymeric matrix. A single membrane stage generally yields only 50–70% CO_2 purity, which is low compared to other technologies [54].

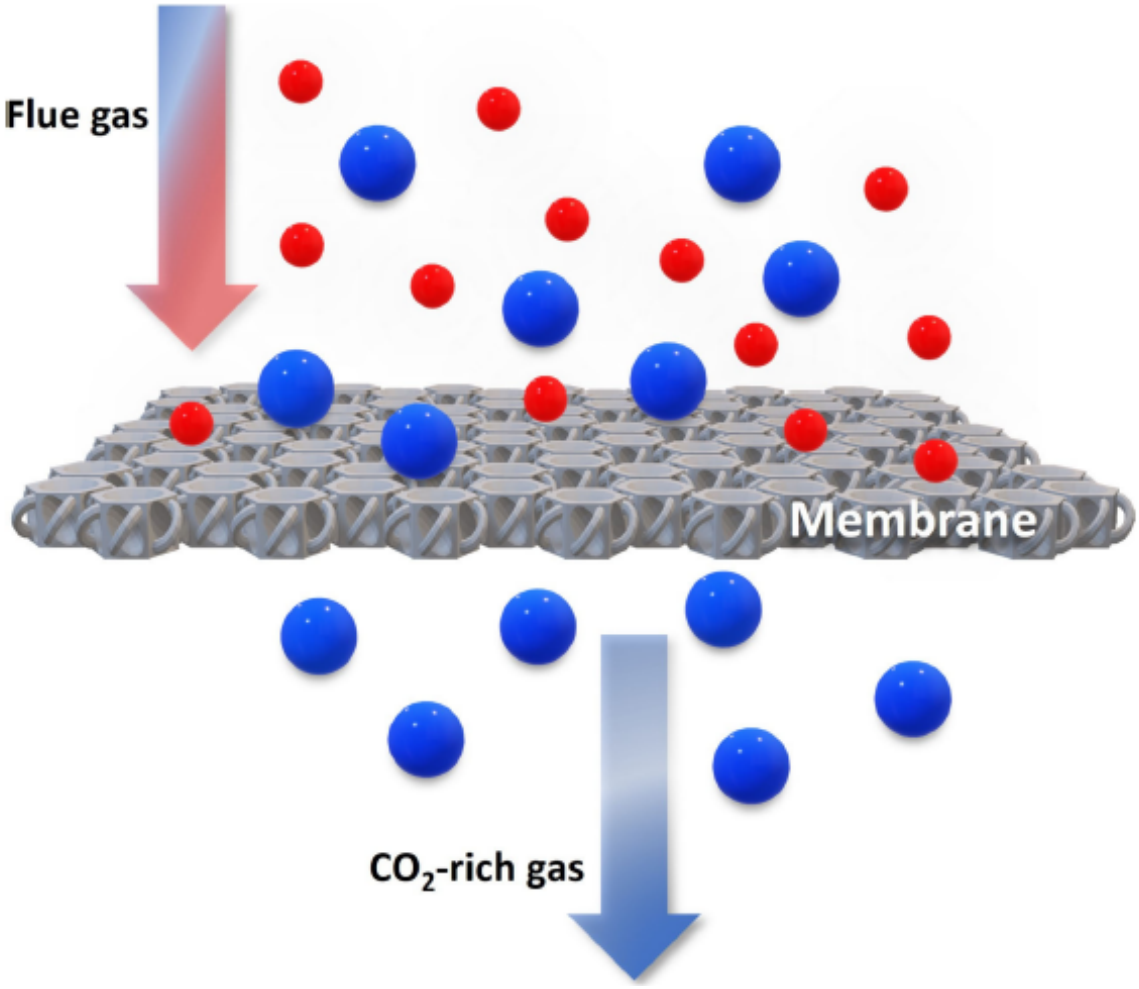

Figure 14: Representation of membrane-based carbon capture [54]

3.4.3.5 Cryogenic separation

Cryogenic separation principle relies on the condensation temperature difference between CO_2 and the other flue gas components (primarily N_2 and O_2). The sublimation point of CO_2 at atmospheric pressure is -78.5°C, while N_2 and O_2 stay in gaseous form down to -196°C and -183°C, respectively ;[54]. The cryogenic carbon capture process cools flue gas to temperatures between -100 and -135°C to turn CO_2 into a solid, separating it from light gases in a recuperative heat exchanger [54]. The solid CO_2 is then compressed to a liquid state at 100–200 bar, directly suitable for pipeline transport for geological storage without additional compression. The exceptional CO_2 purity (>99.9%) and high recovery rates (90–99%) are the main advantages of cryogenic separation. Moreover, the liquid

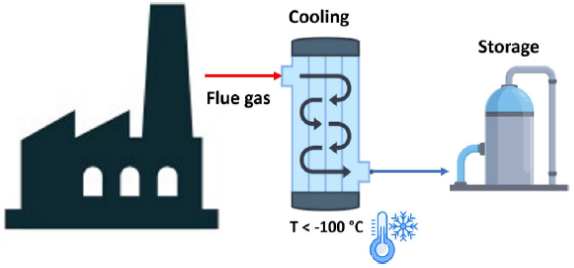

Figure 15: Representation of cryogenic carbon capture [54]

CO_2 produced is directly conditioned for transport and storage, eliminating an additional compression step. However, energy consumption is the primary limitation. It is the most interesting when the flue-gas is already more concentrated in CO_2.

4 Methodology

For the realization of this thesis, the methodology of superstructure optimization is used, similarly to what has been done in the master thesis of Rafailia Mitraki [57]. To apply this methodology, a literature review and data collection step is necessary for model development. The data for raw materials requirements and energy demand used in the models are coming from different sources and represent the most widely implemented processes according the best available techniques in Europe. These data have been validated by the industry to ensure the relevance of the modelling hypothesis.

This section will start with an explanation of OSMOSE, the tool used for the modelling. After that, each model will be presented in details. The base case of the study is the conventional EAF stainless steel production route using only scrap as raw material. The three main steps are the electric arc furnace, the argon oxygen decarburization and the casting and hot rolling. The annual production is fixed at 2.8 million tons of hot rolled stainless steel, based on APERAM presentation booklet available online [58]. In addition to the base case, a few alternative production routes have been considered, including fuel switching and CO_2 capture.

4.1 OSMOSE

OSMOSE (OptimiSation Multi-Objectifs de Systèmes Énergétiques intégrés', i.e. Multi-Objective Optimization of Integrated Energy Systems) is a Lua-based tool developed by the IPESE group of EPFL, Ecole Polytechnique Fédérale de Lausanne. Its goal is to offer decision making support in the improvement of processes by combining databases, optimization methods and solvers, simulation tools and post-analysis methods [59]. The structure of the framework is presented in Figure 16.

The frontend is the file where the solving routine is launched and the problem is defined. The objective function and the choice of the solver and its settings are specified. In this case, the objective is to minimize the total cost of the process. The loading of the different models is also present, along with values of general parameters and post-compute functions [59].

The ET models are the representation of processes that convert the materials and energy inputs into products, by-products, waste or energy [59]. These models consist of four elements:

- Unit: modelled system that is described by its energy and mass balances as well as its cost;
- Streams: material, electricity or energy that enters or exits the unit;
- Layers: specification of the streams that allow the different units to be connected with each other;

- Parameters: used for the definition of the streams or units (cost, temperature, size,...).

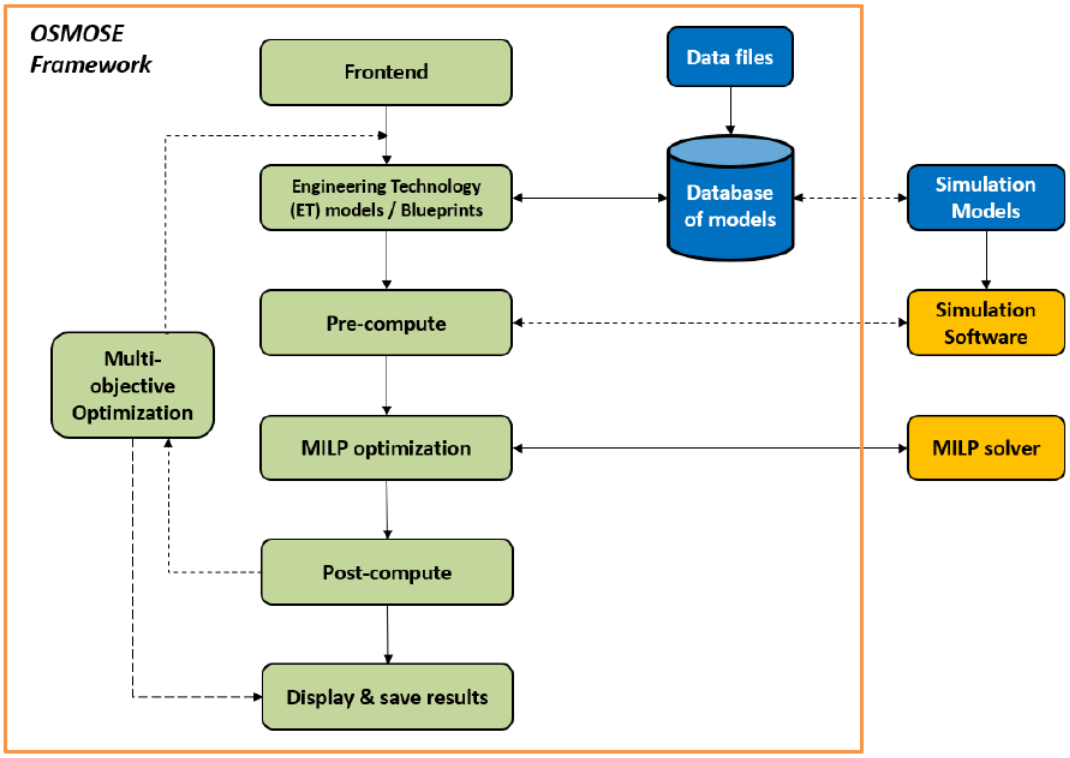

Figure 16: Osmose framework, redraw from redraw from [57] base on [59]

ET models can be linked to an already existing simulation, from Aspen for example. By assembling multiple ET models, a superstructure is obtained, showcasing the totality of a process.

The pre-compute module is used to execute all the computation necessary for the problem optimization. For example, the fuel consumption of a boiler can be determined based on its heat production and efficiency [59].

Once all required parameters have been established, the Mixed-Integer Linear Programming (MILP) optimization can be carried out. The structure of the optimization module is presented in Figure 17. All the ET models are included in a data structure that is then sent to the solver as input files: .MOD files for the equations and .DAT for the parameters. These two types of files are provided to the MILP solver, which will proceed with the optimization and produce the .OUT files with the obtained results. These will serve as input for the post-compute module where several key performance parameters can be calculated [59].

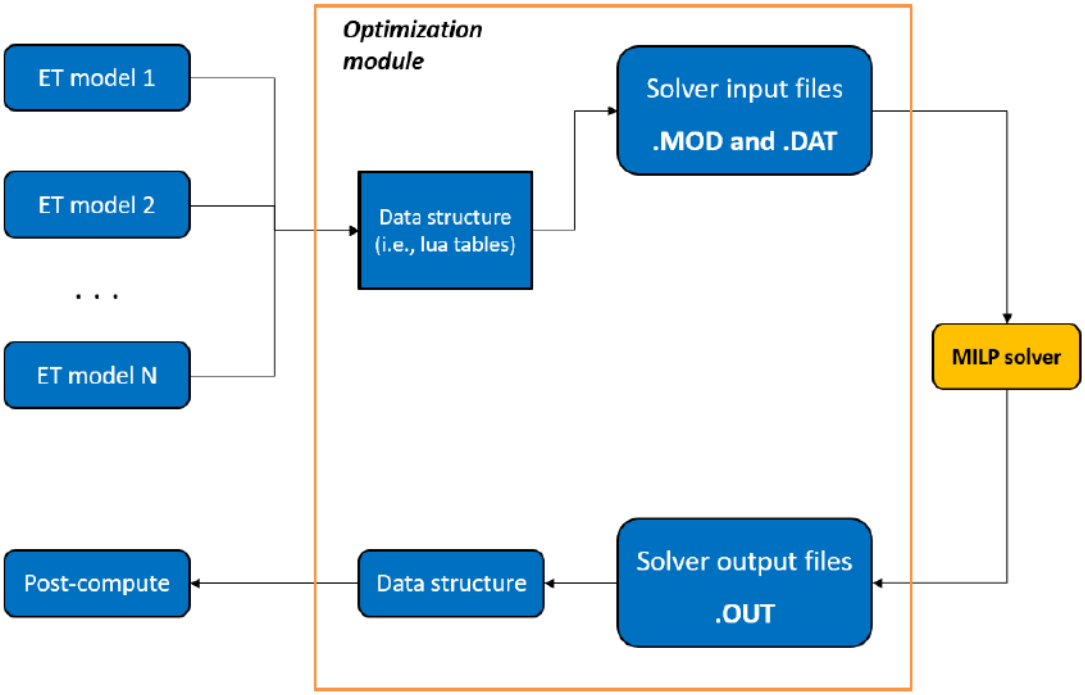

Figure 17: MILP optimization, redraw from [57] base on [59]

OSMOSE also offers the possibility to perform multi-objective optimizations. In this case, the optimization is structured as a master-slave architecture, as shown in Figure 18. The slave optimization consists of a mono-objective MILP problem and is managed by the master optimization [59]. The slave optimization generates a solution that is passed to a post-compute function, which evaluates the values of the objectives considered by the master optimization. Based on these results, the master optimization iteratively updates and resolves the slave problem until convergence is reached for the multi-objective problem.

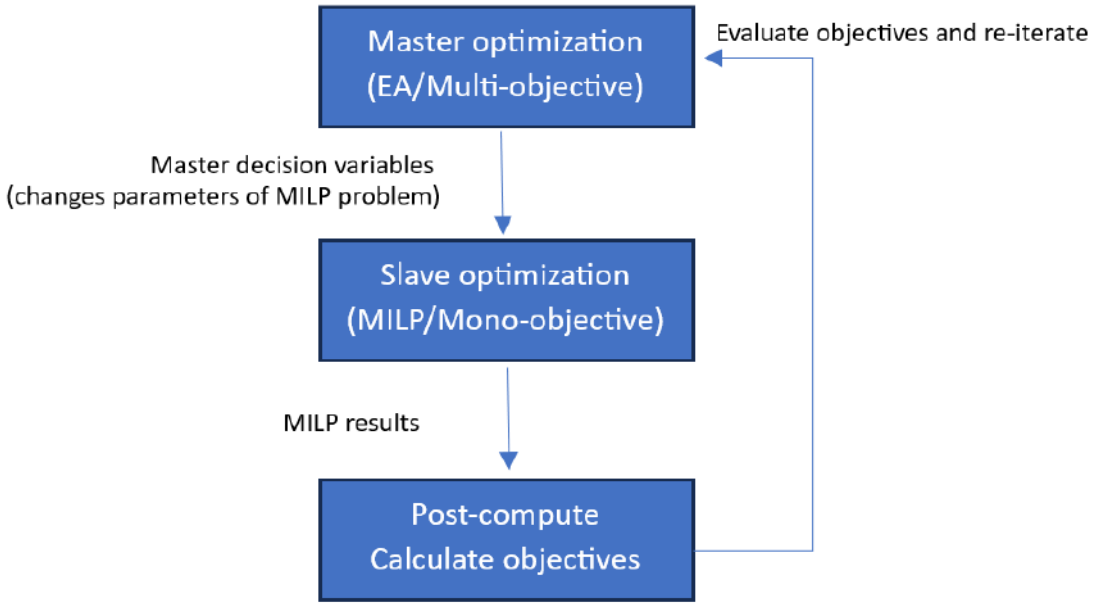

Figure 18: OSMOSE multi-objective optimization, redraw from [57] base on [59]

4.2 Modelling of the electric arc furnace

The black box model of the first step of the process, i.e the electric arc furnace, is presented in Figure 19. As a starting point, the article from Kirschen et al. (2002) is used [60]. This study was the most detailed one found on stainless steel production with scrap and no carbon injection for slag foaming. It considers that scrap is introduced with alloys and slag former. The alloys include ferro-chromium with 50% Cr and ferro-silicium with 75% that are prepared with 9% of Fe-Si and 91% of Fe-Cr [12]. As this study is quite old, it was assumed that progress had been made concerning the fuel burners inside the furnace. Hence, only the mass balance was used for the model.

The energy balance for the furnace has been set based on a more recent article from the same authors [17], considering the electrical energy provided by the electrodes, the energy provided by oxy-fuel burners and the energy released by the main oxidation reactions identified in [17].The ones taken into account were involving the metals present in the simplified composition of [12] and shown to be reacting in that same article. They are presented from Equation 14 to Equation 17.

$$Si + O_2 \longrightarrow SiO_2 \; ; \; \Delta H = -8.94\text{kWh/kg}_{Si} \tag{14}$$

$$Mn + 0.5O_2 \longrightarrow MnO \; ; \; \Delta H = -1.93\text{kWh/kg}_{Mn} \tag{15}$$

$$C + O_2 \longrightarrow CO_2 \; ; \; \Delta H = -8.10\text{kWh/kg}_{C} \tag{16}$$

$$2Cr + 1.5O_2 \longrightarrow Cr_2O_3 \; ; \; \Delta H = -3.05\text{kWh/kg}_{Cr} \tag{17}$$

Oxy-fuel burners are assumed to be fired with natural gas. The required fuel volume is determined based on its lower heating value. Finally, the oxygen to be injected takes into account the oxygen necessary for natural gas combustion and the oxidation reactions inside the furnace [12]. The stoichiometric value was corrected by considering the infiltrated air inside the furnace and the oxygen excess derived from the composition analysis of the off gas [60]. Table 1 summarizes the values of the different model parameters.

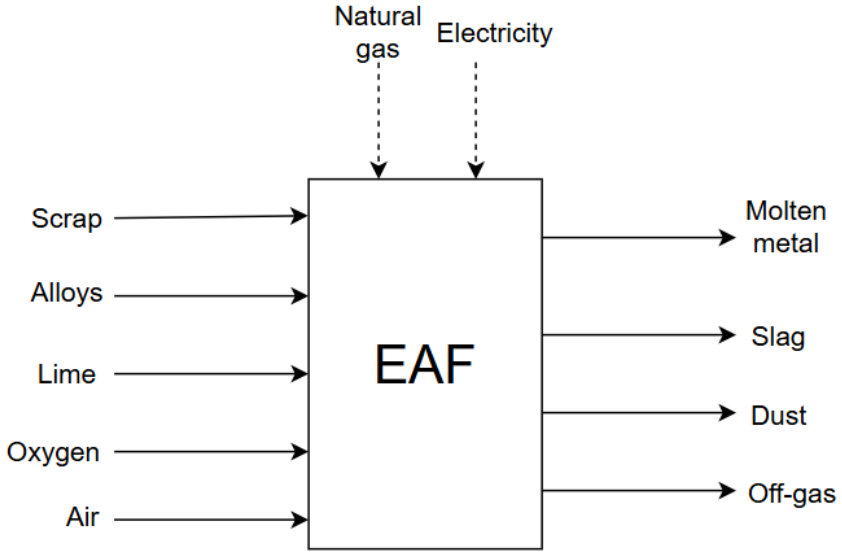

Figure 19: Black box model of the EAF

Table 1: Parameters of the electric arc furnace model

IN		OUT	
Scrap (kg/t steel)	981	**Off-gas (kg/t steel)**	293
Alloys (kg/t steel	125	**Slag (kg/t steel)**	79
Slag former (kg/t steel)	44	**Dust (kg/t steel)**	11
Natural gas (Nm3/t steel)	3,5		
Electrode (kg/t steel)	2,5		
Refractory (kg/t steel)	0,9		
Oxygen (Nm3/t steel)	14		
Infiltred Air (kg/t steel)	267		
Electrical energy (kWh/ t steel)	450		
Energy from NG (kWh/ t steel)	37,5		

4.3 Modelling of the argon oxygen decarbonizer

For the black box model of the AOD that is showed in Figure 20, the article from Tian et al. was used [61]. It was considered that the hot metal coming from the EAF is introduced into the AOD converter with ferro alloys and lime. Moreover, oxygen, argon and nitrogen are injected. In the end, steel is obtained alongside slag, off-gas and dust. The composition

of the off-gas was assumed to be 55.7 % CO_2, 28.1% N_2, 12.1% Ar and 4.3% O_2 by assuming that 9% of O_2 does not react. The summary of the data is presented in Table 2.

Table 2: Model parameters of the AOD model

IN		**OUT**	
Hot metal (kg/t steel)	801	**Steel (kg/t steel)**	1000
Alloys (kg/t steel)	264	**Slag (kg/t steel)**	131
Lime (kg/t steel)	101	**Off-gas (kg/t steel)**	180
Oxygen (Nm^3/t steel)	61	**Dust (kg/t steel)**	9
Argon (Nm^3/t steel)	12		
Nitrogen (Nm^3/t steel)	41		

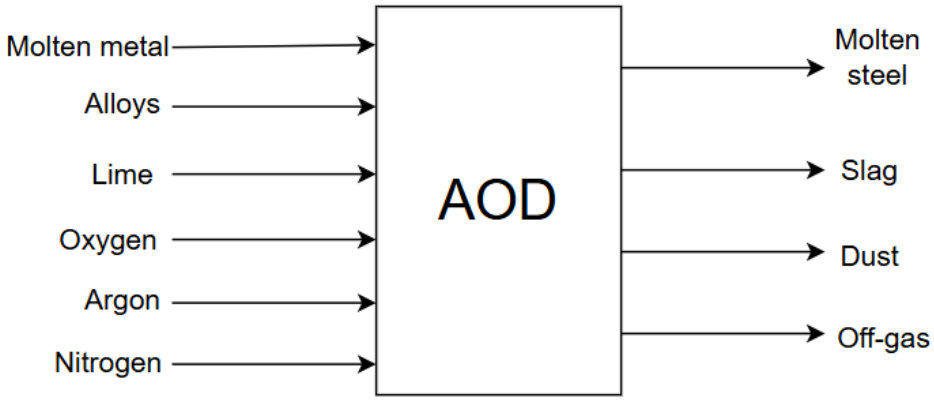

Figure 20: Black box model of the AOD

4.4 Modelling of the continuous casting and hot rolling

The last step of the model concerns the combined continuous casting and hot rolling of the steel. For this part, it was considered that only energy to heat the steel and electricity to run the line was necessary. For easier modelling, casting and hot rolling were combined into a single step that is presented in Figure 21. The data for the energy demand of the continuous casting were found in Khalid et al. [27], whereas the study of Zabik et al.[62] was used for the modelling of hot rolling. For the heat provided by natural gas, the volume of gas was determined using the same heating value as before, while the volume of oxygen assumes a stoichiometric combustion reaction. The off-gas is assumed to be 55% CO_2 and 45% water.The summary of model parameters is presented in Table 3.

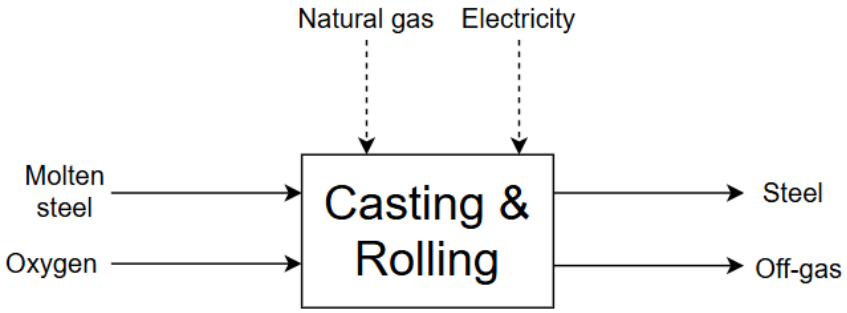

Figure 21: Black box model of casting and hot rolling

Table 3: Model parameters of the casting and rolling model

IN		OUT	
Oxygen (Nm³/t steel)	66	**Off-gas (kg/t steel)**	118
Natural gas (Nm³/t steel)	33		

4.5 Modelling of the alternative routes

For the comparison with emission mitigation pathways, two alterations were considered: fuel switching and carbon capture. For the first one, biomethane and hydrogen were used to replace the natural gas required in the electric arc furnace and in the reheating furnace for the hot rolling step. For carbon capture, absorption with monoethanolamine (MEA) was considered.

4.5.1 Modelling of the fuel switching

To model the different cases of fuel switching, it was considered that everything was kept the same apart from the fuel. The volume of biomethane or hydrogen was determined knowing the energy required by the process step and the heating value of the fuel (30.32 MJ/Nm^3 of biomethane [48] and 10.8 MJ/Nm^3 of hydrogen[50]). The oxygen input was also corrected to match the needed amount for oxy-fuel combustion. The fuel consumption values used in the model are presented in Table 4 and the total oxygen consumption of said model is shown in Table 5. The black box models are schematically represented in Figure 22 for the EAF and Figure 23 for casting and hot rolling.

Table 4: Fuel consumption for the EAF and casting and rolling steps in the fuel switch model

	EAF	**Casting and rolling**
Biomethane (Nm³/t steel)	4.5	43
Hydrogen (Nm³/t steel)	12.5	121

Table 5: Oxygen volume used in the EAF and casting and rolling model with fuel switch

Oxygen volume (Nm^3/t steel)	EAF	Casting and rolling
Biomethane combustion	15,90	86,15
Hydrogen combustion	13,25	60,52

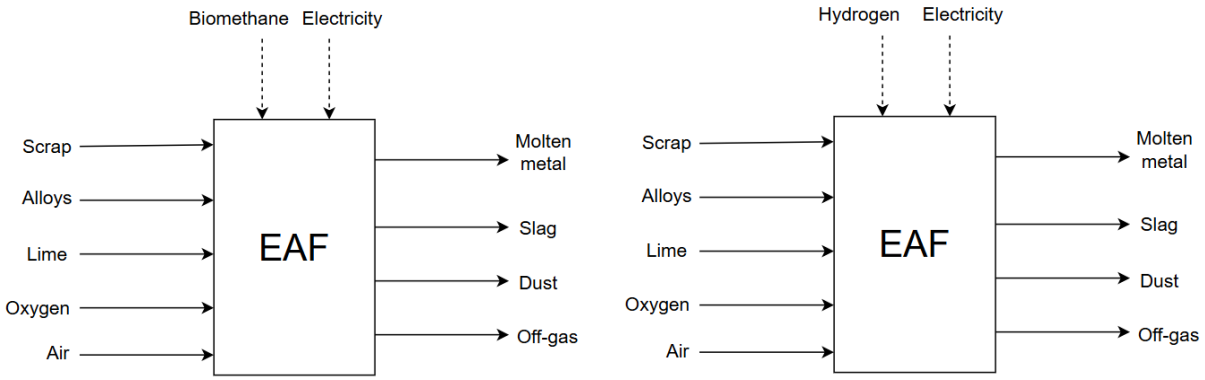

(a) Biomethane (b) Hydrogen

Figure 22: Fuel switching - Black box models of the EAF

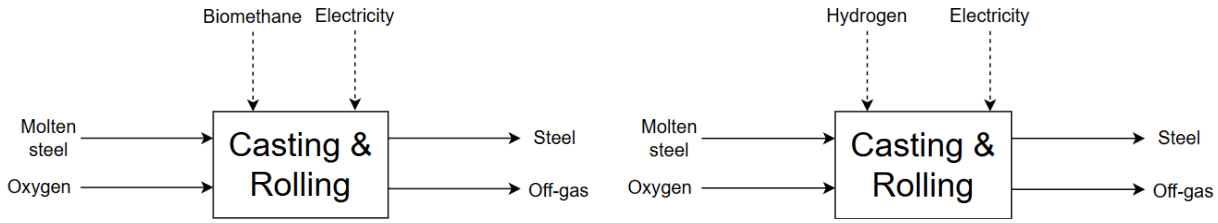

(a) Biomethane (b) Hydrogen

Figure 23: Fuel switching - Black box models for casting and rolling

4.5.2 Modelling of the carbon capture

From the carbon capture technologies presented in the literature review, it has been chosen to implement chemical absorption with MEA due to its technical maturity. The model described in this section has been developped by Rafailia Mitraki and used in her Master's thesis [57]. A black box diagram for the carbon capture unit is presented in Figure 24. It consist of two blocks: the capture and the compression.

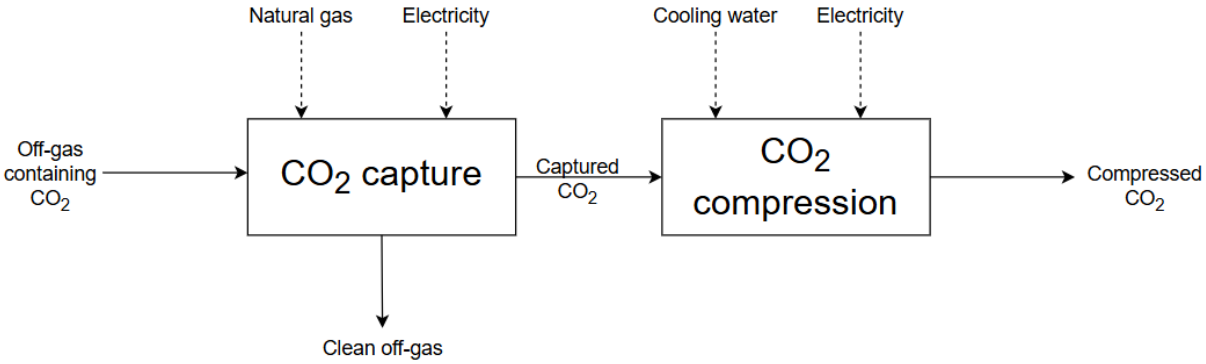

Figure 24: Black box model of the CO_2 capture and compression unit

The capture of CO_2 with MEA is described in Figure 25. The mixed off-gas coming from the EAF, AOD and hot rolling steps is first cooled down to 40°C before entering the absorption column. Inside the column, MEA selectively absorbs the CO_2 and the purified gas is leaving at the top. The amine solution that is charged with CO_2 will be preheated by the regenerated solution coming from the desorption column before entering this second column. The pure CO_2 exits at the top at 101°C before getting cooled down, whereas the MEA solution is sent back to the first column.

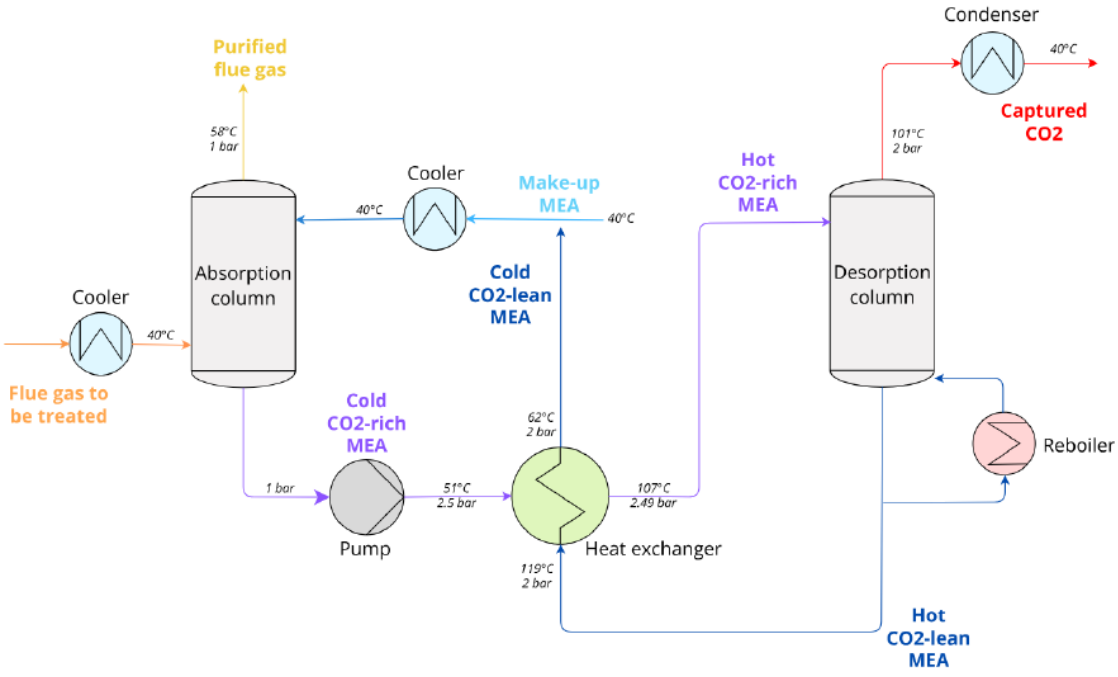

Figure 25: CO_2 capture process with MEA [57]

Once CO_2 has been isolated, it undergoes compression to be safely stored. This compression step is schematically represented in Figure 26.

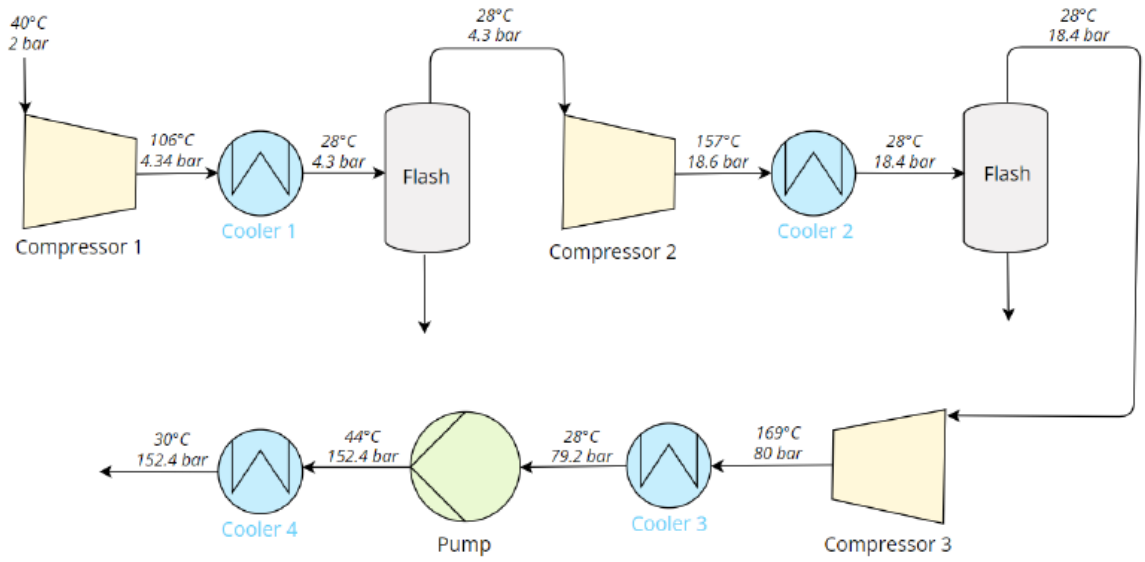

Figure 26: CO_2 compression process [57]

The CO_2 that is at 40°C and 2 bar, coming from the desorption column, will be compressed in four stages. First, the pressure is increased to 4.3 bar. A cooling to 28°C is operated to be able to separate the condensed water using a flash. The second compressor elevates the pressure up to 18.6. It is once again followed by a cooling and a flash to remove condensed water. Using a third compressor, the pressure rises to 80 bar. Finally, the CO_2 is compressed to 152 bar before being cooled down at 30° and leaving the unit.

The energy requirements in the carbon capture unit are electricity for the pump and compressors, cooling water for the cooling and steam produced by a natural gas boiler for solvent regeneration. They are calculated for each case where applicable, along with the investment cost, based on the correlations established by Kim et al. [63]. These correlations depend on the gas flow rate and the CO_2 concentration. In the model, the efficiency of the capture is considered to be 90%. The flow of treated off-gas is equivalent to the sum of each off-gas coming from the EAF, the AOD and the casting and rolling, around 590 kg/t steel for the natural gas model and 627 kg/t stell for the biomethane model. The fraction of CO_2 in these mixed fumes has been calculated for both natural gas and biomethane configurations. It is respectively 0.24 and 0.25.

4.6 Cost evaluation

4.6.1 CAPEX

Due to lack of data for the cost evaluation of EAF, AOD or rolling, it was chosen to only consider the cost of the specific burners as it can be assumed that they will be the only modifications between the modelled alternatives. Based on a report on industrial fuel

switching [64], the price for each type of burner was determined using Equation 18.

$$CAPEX(€) = Reference\ CAPEX(€/kW) \cdot Size(kW) \cdot \left(\frac{Size(kW)}{Reference\ Size(kW)}\right)^{0.6} \quad (18)$$

The CAPEX can be annualized over its lifetime using the Equation 19.

$$\text{Annualized CAPEX} = CAPEX \cdot \left(\frac{i(1+i)^n}{(1+i)^n - 1}\right) \quad (19)$$

In this case, i is the discount rate (fixed as 8.5%) and n is the lifetime of the which is chosen to be 30 years.

Knowing the production capacity and the energy requirement of the process, the cost of the burner of adequate size was determined for the EAF and rolling step for each configuration. For both natural gas and biomethane, the same burner cost is taken into account for the calculation as the composition of the fuels are very similar. The summary of the cost for each case is presented in Table 6

Table 6: Annualized cost of burners for different fuels

	Natural gas & biomethane	**Hydrogen**
Burner price (€)	4 329 119	7 494 120

4.6.2 OPEX

For the evaluation of the operational expenditure, the components considered are the cost of raw materials, electricity, fuel and the cost of CO_2 emissions based on the European Emissions Trading System (EU ETS). Equation 20 is used for the computation of the OPEX for each case. The costs per specific unit are displayed in Table 7 with their sources.

$$OPEX(€) = \sum_i C_{RawMat(i)} \cdot m_{RawMat(i)} + C_{Elec} \cdot E_{Elec} + C_{Fuel} \cdot V_{Fuel} + C_{CO_2} \cdot m_{CO_2} \quad (20)$$

Where C_{RawMat} is the cost of a specific raw material per kg, $m_{RawMat(i)}$ is the mass of the specific raw material, C_{Elec} is the cost of electricity per kWh, E_{Elec} is the electrical energy demand, C_{Fuel} is the cost of the specific fuel per Nm^3, V_{Fuel} is the required volume of fuel, C_{CO_2} is the CO_2 ETS price and m_{CO_2} is the mass of CO_2 emitted by the process.

Table 7: Specific cost for different commodities

Material	Price	Source
Steel scrap (€/kg)	0.48	[65]
Lime (€/kg)	0.18	[66]
Alloys (€/kg)	2.22	[67]
Oxygen (€/Nm³)	0.28	[68]
Argon (€/Nm³)	1.10	[69]
Nitrogen (€/Nm³)	0.22	[70]
Natural gas (€/Nm³)	0.52	[71]
Biomethane (€/Nm³)	0.71	[72]
Hydrogen (€/Nm³)	0.81	[73]
Electricity (€/kWh)	0.18	[74]
CO_2 tax (€/kg)	0.075	[75]

4.7 Price scenario evaluation

With new regulations about fossil fuels use and more and more industries interested in the development of greener processes, it is certain that energy prices will evolve. To be able to make this study relevant in a larger scope than the current situation, three scenarios are proposed for the energy prices : the current scenario called "2026", an optimist price scenario called "ideal" and a third scenario called "competition" [76].
The first scenario is developed based on current energy prices. Electricity is relatively expensive and priced at 185€/MWh [71]. Natural gas is the cheapest fuel, costing only 47€/MWh [71]. Hydrogen cost is relatively high as only green hydrogen produced by water electrolysy. It is currently estimated at 270€/MWh [73]. Biomethane price lies between the ones of electricity and natural gas, at 85€/MWh [72]. The CO_2 is fixed at its current ETS price, 0.075 €/kg CO_2 [75].

In the ideal scenario, prices are adapted to favor low carbon configurations. Natural gas price is increased while most of the other prices are reduced. Biomethane price is very similar to natural gas but still slightly cheaper, with respectively 54 [72] and 55€/MWh. Electricity only costs 95€/MWh [77]. Hydrogen price decreases, placing at 100€/MWh because of the assumption that cheap clean hydrogen is imported to Belgium. The CO_2 tax has massively increased to drive an increase of investment in renewable energy, up to 0.3 €/kg CO_2 [78].

Finally, the competition scenario represents a more realistic adaptation of the ideal one. The natural gas price remains the same but other prices have increased. As more industries will be tempted to use alternative fuels and renewable energy, their access will become more difficult as the amount available will be too low for everyone [79]. This will result in a market with a larger competition, thus higher prices. In this scenario, electricity costs 111€/MWh, hydrogen 135€/MWh and biomethane 168€/MWh [78].
A summary of these three scenarios is presented in Table 8.

Table 8: Energy price scenarios

	2026	Ideal	Competition
Electricity price (€/MWh)	185	95	111
Natural gas price (€/MWh	47	55	55
Biomethane price (€/MWh)	85	54	168
Hydrogen price (€/MWh)	270	100	135
CO_2 tax (€/kg CO_2)	0.075	0.3	0.2

4.8 Indirect emissions evaluation

As the direct, or scope 1, emissions are calculated by the model, the indirect, or scope 2, emissions can also be accounted for a more complete evaluation. In this report, only the indirect emissions for the electricity and fuel production are considered. The ones related to the raw materials production are excluded since they'll remain identical across all configurations.

Scope 2 emissions are calculated by using Equation 21.

$$\text{Scope 2 emissions (kg } CO_2\text{/t steel)} = \sum_i EF_i \cdot E_i \tag{21}$$

Where EF_i is the emission factor associated to the energy vector i in kg CO_2/kWh and E_i is the energy demand in i type of energy in kWh/t steel.

Two periods of evaluation are considered, namely the current situation in 2026 and a forecast for 2050. The latter is used when the ideal and competition energy pricing scenarios are analysed. The emission factors for electricity, natural gas, biomethane and hydrogen are presented in Table 9.

Table 9: Indirect emissions for different energy vectors

Fuel	**Indirect emissions (kg CO_2/kWh)**	
	2026	**2050**
Natural gas	0.039	0.039
Hydrogen	0,220	0,093
Electricity	0.138	0.058
Biomethane	0.036	0.036

For natural gas and biomethane, they remain the same for both scenario. For hydrogen, the emission factor highly decreases because of the evolution of the electricity grid mix. For electricity, the factors are deducted from the current carbon intensity of the Belgian grid [80] in the 2026 scenario. For the supposed 2050 scenario, the projected electricity mix in Europe [81] with the emission factor for each type of electricity production coming from Ecoinvent are used to compute the mean impact of electricity use using Equation 22.

$$EM_{e,2050} = \sum_i E\%S_i \cdot I_i \tag{22}$$

Where $EM_{e,2050}$ is the emission factor for electricity use in 2050, $E\%S_i$ is the share in the mix of electricity produced via source i and I_i its impact

Table 10 presents the share of each electricity production and their associated emission factor with the detail of the sources.

Table 10: European electricity mix breakdown with associated emission factor in the 2050 scenario

Type	%	kgCO2/kWh	Sources
Wind onshore	31,7%	0,019	Average of [82] and [83]
Wind offshore	24,5%	0,015	[84]
Solar	33,1%	0,092	Average of [85], [86] and [87]
Other RES	2,0%	0,064	[88]
Hydro and pumped storage	4,6%	0,322	[89]
Nuclear	3,6%	0,006	[90]
Methane	0,4%	0,501	Average of [91], [92], [93] and [94]

As electricity is a dominant energy source in the EAF, the emission factors for renewable electricity production by solar panels [85],[86],[87] and wind turbines [82], [83] are also considered separately to compare them to the Belgian electricity mix, in case the production plant could be able to have its own on-site electricity production.

5 Results and discussions

5.1 Superstructure development

The superstructure of the stainless steel production via EAF and its alternatives is presented in Figure 27.

In this superstructure, molten metal is produced via the scrap-based EAF route, which is then treated in a AOD unit. Finally, the stainless steel product of the desired shape is obtained after casting and hot rolling. In the base case, natural gas is used as an additional energy vector in the EAF, while natural gas combustion provides the required heat for the hot rolling step.

To reduce emissions, two alternative fuels are considered: biomethane and hydrogen. Moreover, due to the high electricity demand of the process, especially in the EAF, several electricity production routes are considered: electricity sourced from the national grid, as well as renewable electricity produced from wind turbines or solar panels. Finally, the last option of the superstructure consists in the implementation of a carbon capture unit, and more specifically the most mature technology, i.e., MEA-based chemical absorption.

Five different stainless steel production configurations are investigated in this study, depending on the energy resource used and the implementation, or not, of carbon capture. The corresponding abbreviations are listed in Table .

Table 11: Configuration details and abbreviations

Abbreviation	**Configuration details**
NG	Natural gas (NG) is used in the EAF and rolling step
NG+CC	NG is used in the EAF and rolling step, and carbon capture is implemented
BIOCH4	Biomethane (BioCH4) is used in the EAF and rolling step
BIOCH4+CC	BioCH4 is used in the EAF and rolling step, and carbon capture is implemented
H2	Hydrogen is used in the EAF and rolling step

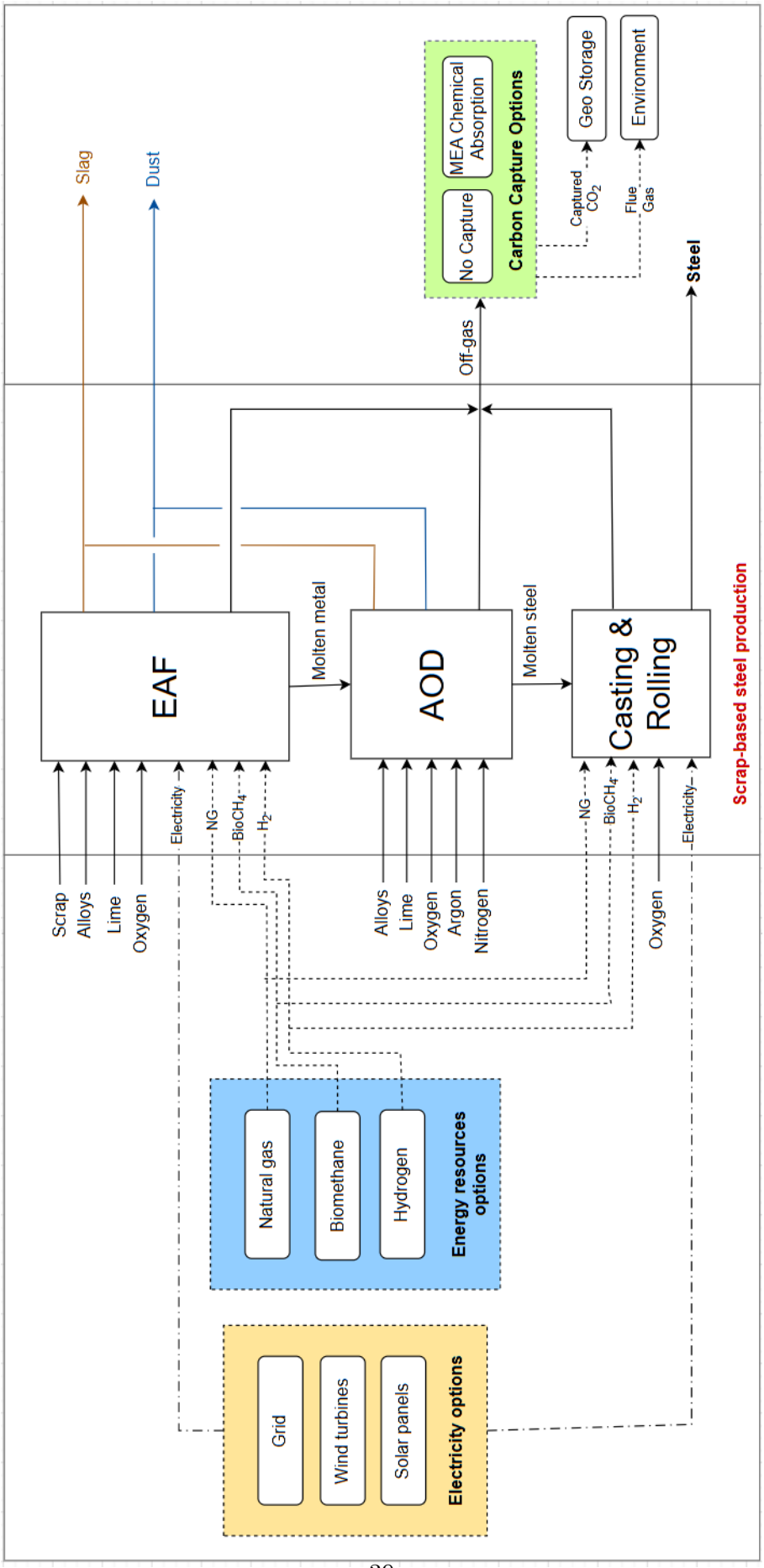

Figure 27: Superstructure of the stainless steel production

5.2 Energy demand and scope 1 emissions

The results in terms of energy demand per source and specific CO_2 emissions for each case is presented in Table 12. Scope 1 emissions range from 15.6 kg CO_2 / t steel in the best case for biomethane with carbon capture ("BIOCH4+CC") to 191.2 kg CO_2 / t steel in the worst case for natural gas ("NG"). Between the extrema lie the cases of biomethane ("BIOCH4") and hydrogen ("H2"), with the corresponding emissions amounting to 121 kg CO_2 / t steel, as well as natural gas with carbon capture ("NG+CC") emitting 22.3 kg CO_2 / t steel. Fuel switching options, such as "H2" and "BIOCH4", result in an emission reduction potential of 37% compared to the base case due to the emissions intrinsic to the oxidation reactions in the metal and the electrodes degradation. Indeed, 9 kg CO_2 / t steel were produced by the electrodes, 11 by the metal oxidation inside the EAF and 101 inside the AOD, adding up to 121 kg CO_2 / t steel Implementation of CO_2 capture in natural gas-fired facilities reduces emissions by 88%. Moreover, CO_2 emissions can be further reduced by combining fuel switching and CO_2 capture, with "BIOCH4+CC" showcasing an emission reduction potential of 93% compared to the base case.

Table 12: Energy demand, scope 1 emissions and emission reduction potential

Cases	Electricity use (kWh/t)	Natural gas use (kWh/t)	Biomethane use (kWh/t)	Hydrogen use (kWh/t)	Scope 1 CO_2 emissions (kg/t)	Emission reduction potential
NG	**375**	**392**	**0**	**0**	**191.2**	-
NG+CC	**392**	**2186**	**0**	**0**	**22.3**	**88%**
BIOCH4	**375**	**0**	**393**	**0**	**121**	**37%**
BIOCH4+CC	**386**	**1956**	**393**	**0**	**15.6**	**93%**
H2	**375**	**0**	**0**	**391**	**121**	**37%**

The electricity and natural gas requirements of each step of the process is presented for the "NG+CC" configuration in Table 13. This case is chosen to be detailed as it will be the same as the conventional "NG" case, to which the energy demand for the carbon capture unit will be added. As it can be seen in the table, the most demanding step regarding electricity is the EAF, with a specific electricity demand of 374.9 kWh/t steel. Concerning the natural gas, the highest consumption is found in the carbon capture unit with 1795 kWh/t steel. When no capture is implemented, the largest natural gas consumer is in the casting and rolling step, which is consistent with what was previously presented in the literature review.

Table 13: Electricity and natural gas requirement for the "NG+CC" case

	Electricity (kWh/t steel)	Natural gas (kWh/t steel)
EAF	374.9	32.1
Casting and rolling	134	359.7
Carbon capture	17.9	1795

5.3 Carbon footprint

Only considering scope 1 emissions is not sufficient for a rigorous analysis. The evaluation of the scope 2 emissions for the 2026 scenario is depicted in Figure 28. For each case, the scope 2 emissions are calculated based on the current electricity mix in Belgium. Moreover, additional emissions arising from fuel extraction or production are also included.

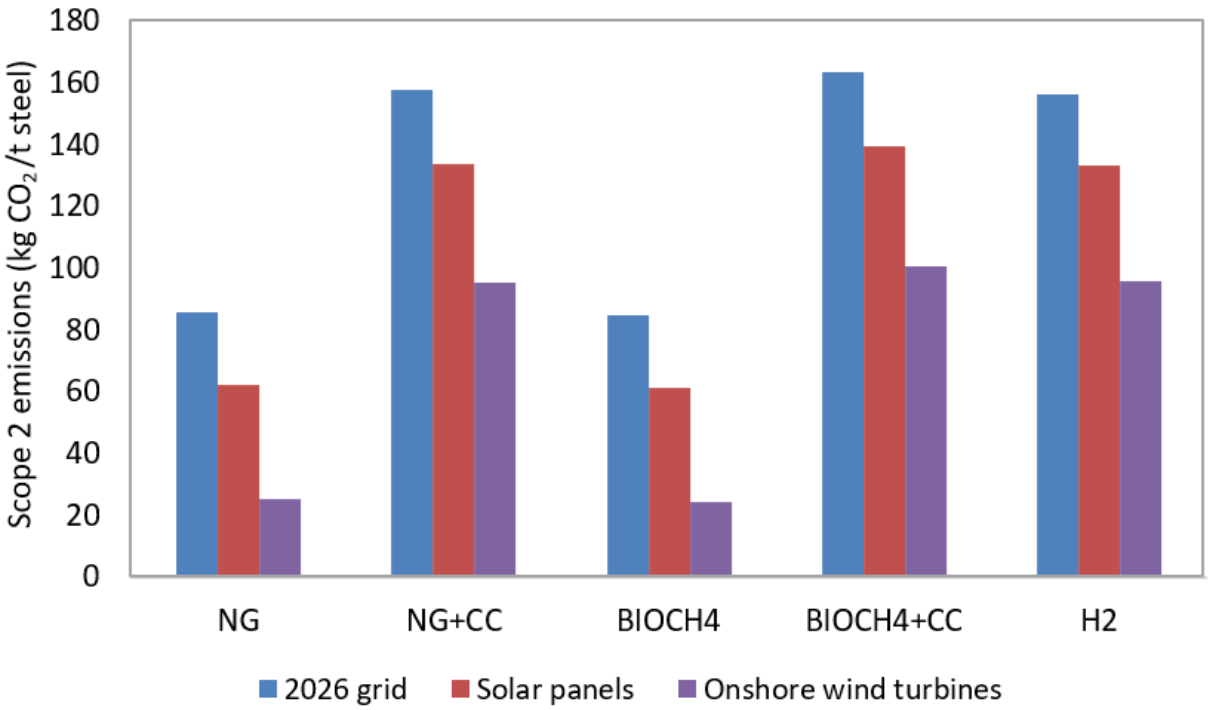

Figure 28: Indirect emissions for all cases in the 2026 scenario

For the current electricity mix, the scope 2 emissions for "NG" and "BIOCH4" are close to each other, amounting for 85 kg CO_2/t steel. They represent the smallest value across all the presented cases. Regarding the "H2" case, the impact is higher than the previous discussed case with 156 kg CO_2 per ton of steel. This can be explained by the energy-intensive hydrogen production, requiring 53 kWh_e/kg H_2 [95]. Regarding the cases with carbon capture, the indirect emissions of "NG+CC" and "BIOCH4+CC" case are the highest of them all with 157 and 163 kg CO_2/t steel, respectively, due to the higher fuel and electricity consumption than the one observed in the other cases.

When considering the production of renewable electricity by solar panels or wind turbines, the impact is drastically decreased for the "NG" and "BIOCH4" cases. This can be explained by the fact that the share of electrical energy compared to fuel energy is bigger in both "NG" and "BIOCH4" configurations, as it can be seen in Figure 29. In fact, as the share of scope 1 and scope 2 from the fuel evolve but not the share of scope 2 from the electricity. It has more influenced on the cases with lower scope 1 emissions.

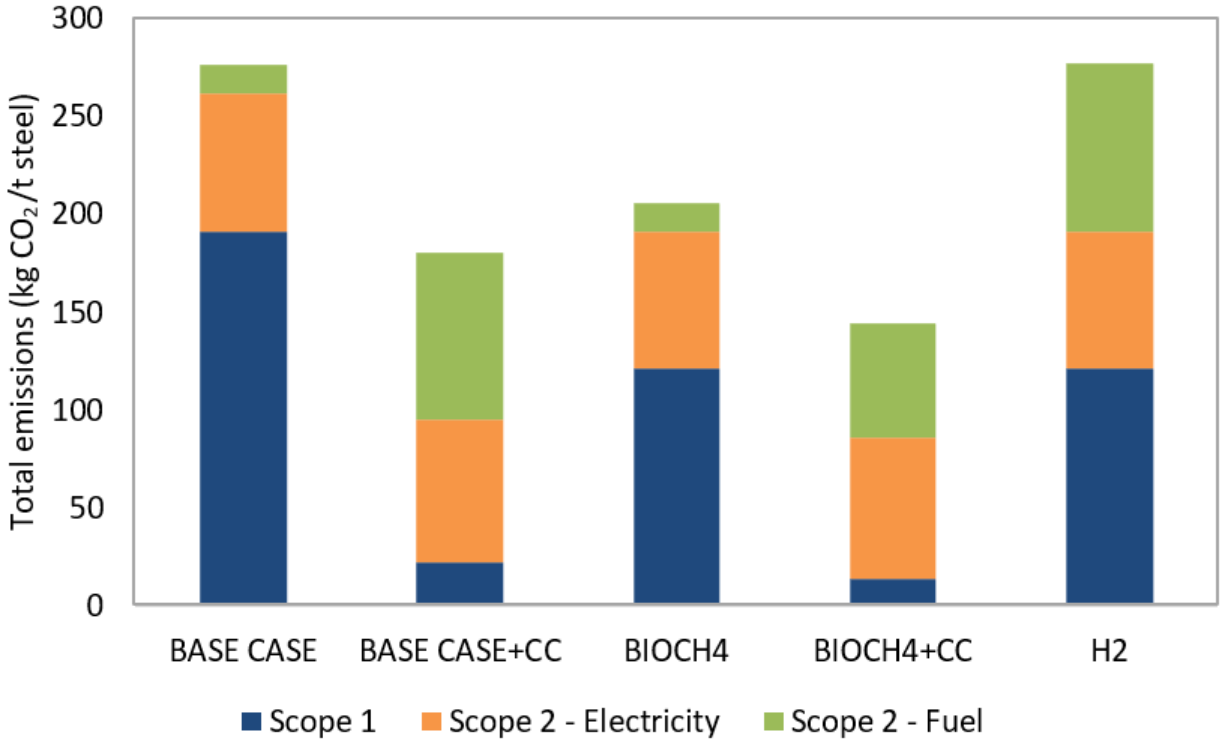

Figure 29: Total emissions breakdown for the 2026 scenario

The sum of scope 1 and scope 2 emissions is shown in Figure 30. When considering total emissions, the best alternatives, from an environmental point of view, are both carbon capture-based cases, with "BIOCH4" being slightly higher. Surprisingly, the impact of "H2" is relatively close to the one of "NG". Electricity produced by wind turbines provides the lowest impact compared to the current electricity mix and the production relying on solar panels.

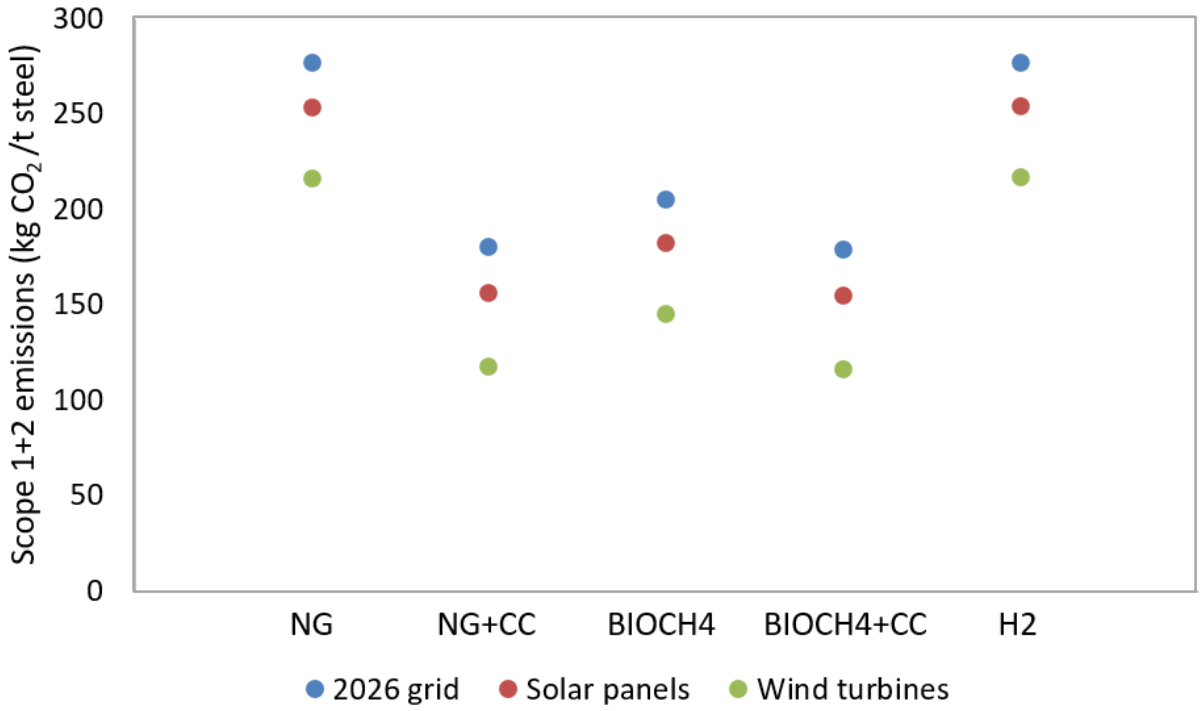

Figure 30: Scope 1 and 2 emissions for the 2026 scenario

In the same way as for the 2026 scenario, the indirect emissions are compared for all configurations using the projected electricity mix for the 2050 scenario. The results are shown in Figure 31. Comparatively to the 2026 scenario, some improvement can be noticed. The pair constituted of the "NG" and "BIOCH4" cases still shows the lowest indirect emissions. These amount to 62 and 61 kg CO_2/t steel, respectively. It corresponds to an improvement of 44% for the "NG" case and 45% for the "BIOCH4" configuration compared to the 2026 scenario. The biggest improvement is recorded for the "H2" case with a 58% improvement, which is associated with scope 2 emissions of 66 kg CO_2/t steel. Finally, the "NG+CC" and "BIOCH4+CC" configurations show the lowest improvement, amounting to only 23% for both of them. They remain the production routes with the biggest scope 2 impact, amounting to 116 and 121 kg CO_2/t steel respectively.

When comparing the different sources of electricity, the ranking presented for the 2026 scenario changes. Wind-based electricity remains the leader but electricity generated by solar panels is overtook by the electricity grid mix in terms of low emissions. As electricity produced by wind turbine represents a larger share in the 2050 electricity mix, its corresponding low impact influences positively the global impact of the grid mix.

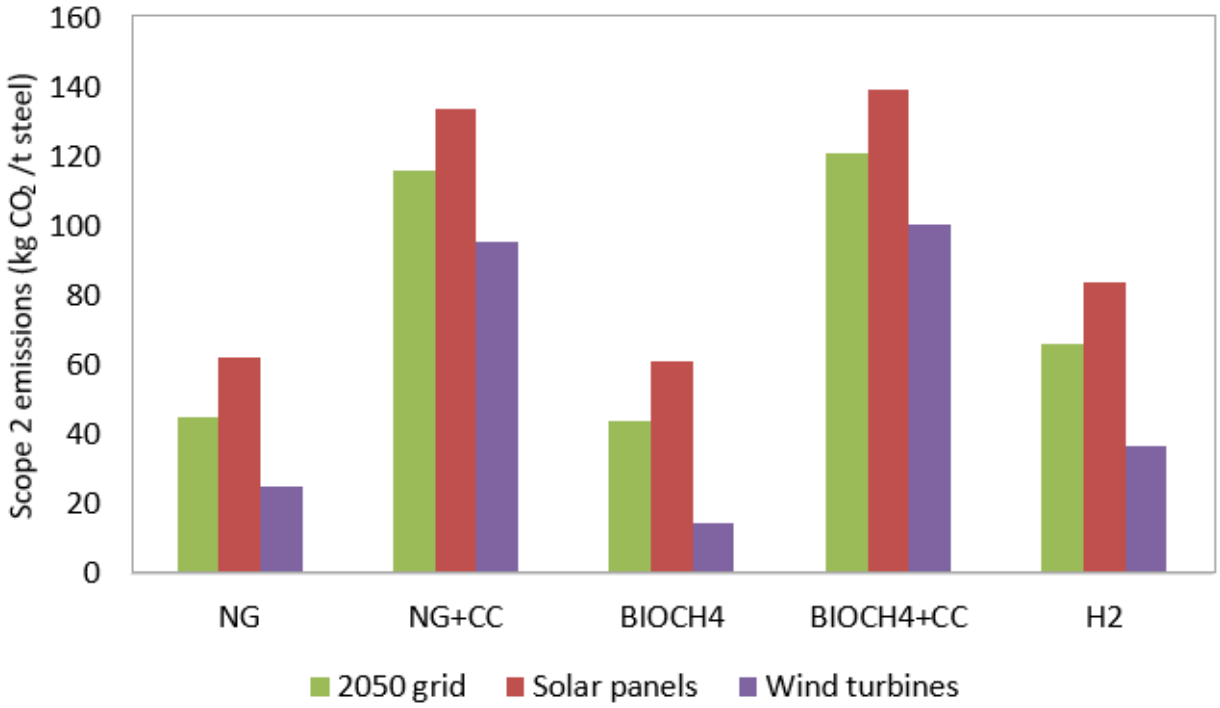

Figure 31: Indirect emissions for all cases in the 2050 scenario

The sum of scope 1 and scope 2 emissions for the 2050 scenario is depicted in Figure 32. The impact of "NG" is the highest among all production configurations investigated. Even if "NG+CC" and "BIOCH4+CC" are still the most interesting from a CO_2 emission perspective, the "BIOCH4" case remains very similar to the former. Moreover, the environmental ranking of "H2" is noticeably improved, with total emissions getting closer to the levels observed for the other alternatives. Wind turbines remain the best electricity production method, since they are characterized by the lowest emission factor. It also contributes to the improved emission factor of the electricity grid mix, which assumes an increased share of wind-based electricity compared to the 2026 scenario.

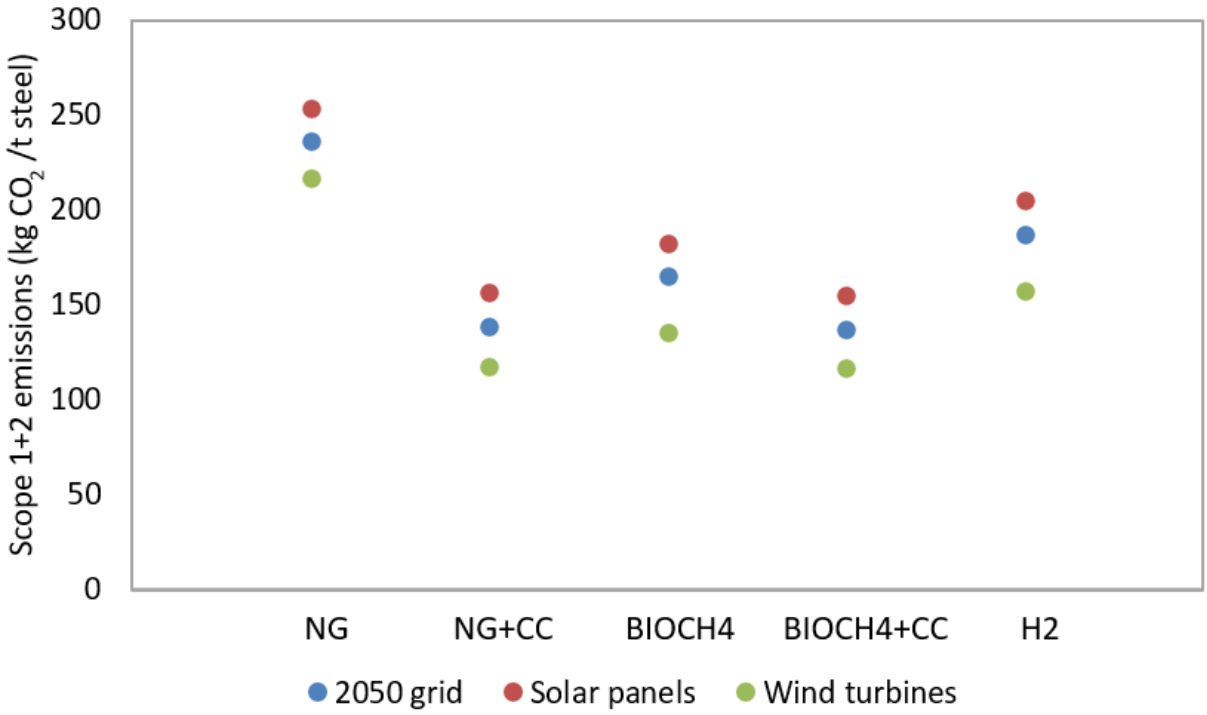

Figure 32: Scope 1 and 2 emissions for the 2050 scenario

5.4 Economical analysis

The breakdown of the cost for all configurations in the 2026 scenario is depicted in Figure 33. It can be observed that the largest share is attributable to the cost of raw materials, amounting to approximately 536€/t steel.

The fuel-related cost is the contribution that varies the most between the different cases. It is usually considerably smaller for the cases without carbon capture. The lowest contribution arises in the "NG" case with 18€/t steel, followed by the "BIOCH4" case with 33 and 105€/t steel. Due to the additional fuel consumption related to the carbon capture unit, the fuel cost contribution becomes more important, amounting to 103€/t steel for the "NG+CC" case and 125€/t steel for the "BIOCH4+CC" case.

On the contrary, the cost contribution of electricity is mostly the same for all cases, between 91 and 95€/t steel. Since the carbon capture unit induces a very small variation for electricity use, the corresponding impact on the cost is limited.

As the CAPEX only takes into account the cost of the burner and the capture unit, it has a limited impact on the total cost. CAPEX contribution varies between 2€/t steel for fuel switching options and 18€/t steel when carbon capture is implemented. Lastly, the cost corresponding to the emission of scope 1 CO_2 represents only a very small share of the total cost, barely visible on this graph. It amounts to 2 to 15 €/t steel, representing between 0.2 and 2% of the total cost. Hence, the current value of the ETS price is not a sufficient incentive for new investments in technologies lowering CO_2 emissions.

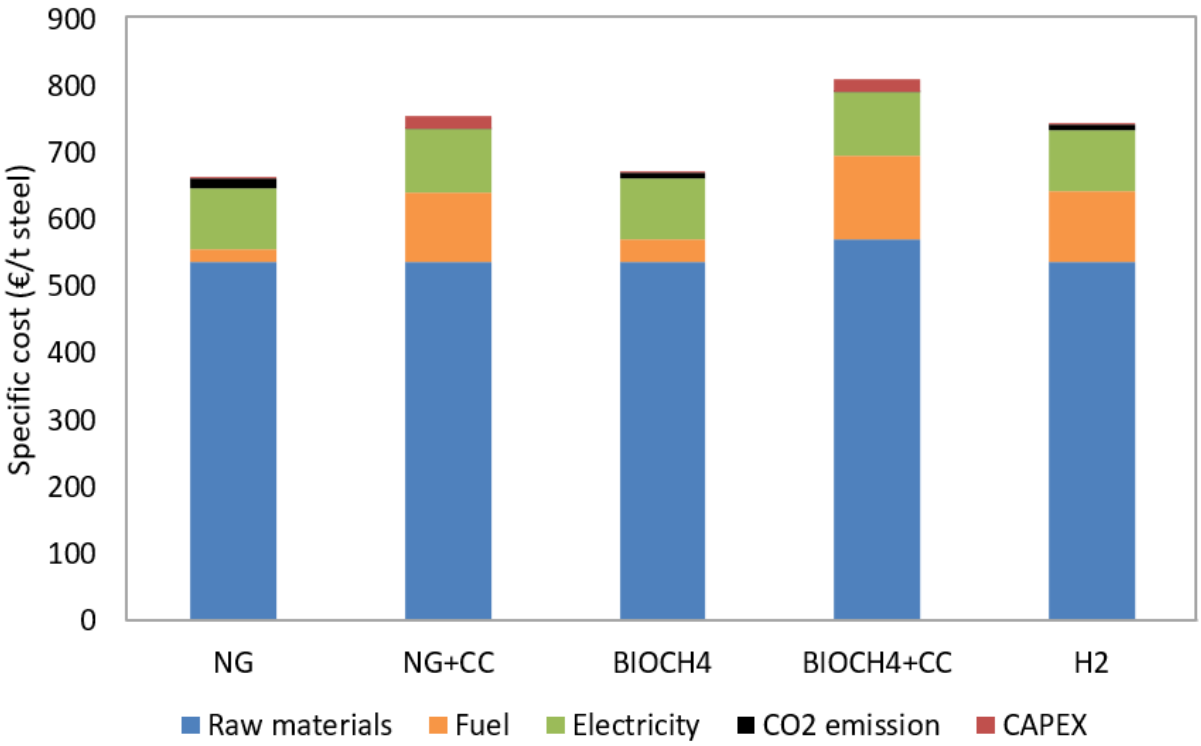

Figure 33: Cost breakdown for all cases in the 2026 pricing scenario

The cost breakdown for the ideal pricing scenario is given in Figure 34. As they did not change from the previous scenario, the CAPEX and raw material costs still account for the same amount in the total cost.

When comparing the "BIOCH4" case with the "H2" and "NG" configurations, the CO_2-related cost and the fuel cost are what determines the cheapest option. In fact, every other cost contribution being mostly the same, the lower emissions in the "BIOCH4" case and the cheaper biomethane price lead to a lower total cost than in any other cases. Despite a natural gas price that is lower than the price of hydrogen, the "H2" configuration is slightly less costly than the base case due to the lower CO_2 cost.

When comparing both alternatives implementing carbon capture, namely "NG+CC" and "BIOCH4+CC", combining fuel switching and carbon capture results in a higher cost than the cost associated with its fossil counterpart. This can be explained by the higher fuel consumption of the former, relating to the heat for the desorption column in the capture unit.

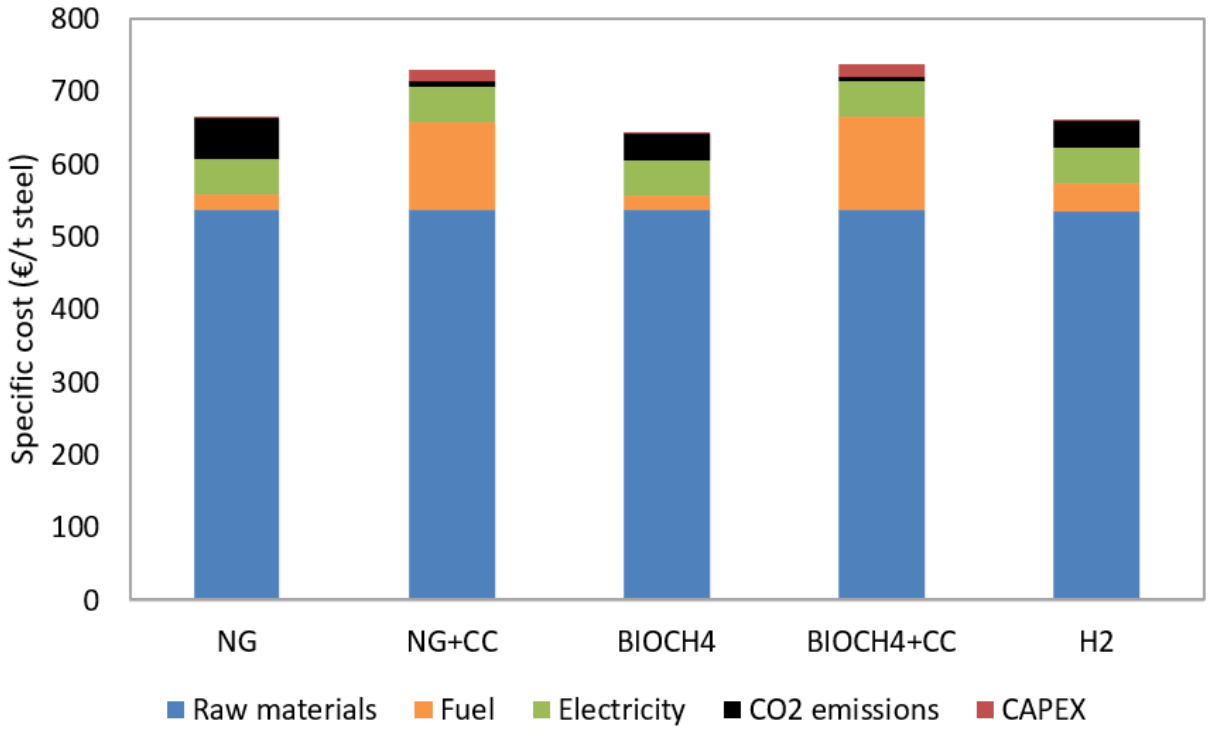

Figure 34: Cost breakdown of all cases in the ideal pricing scenario

For the competition pricing scenario, presented in Figure 35, the breakdown is different. As the price of biomethane increases, the fuel contribution becomes more important in the "BIOCH4" and "BIOCH4+CC" cases. Despite a much higher CO_2 ETS price than currently observed (200 €/t CO_2 vs. 75€/t CO_2 in the 2026 scenario), the low price of natural gas compared to the one of biomethane leads to the base case "NG" being the cheapest production route. Moreover, when carbon capture is implemented, their comparatively high fuel consumption is what renders them more expensive than their counterpart without carbon capture. Finally, cheaper hydrogen allows the "H2" case to become economically competitive with the "NG" case. Their total cost are relatively close even if the "NG" case remains the cheapest route overall.

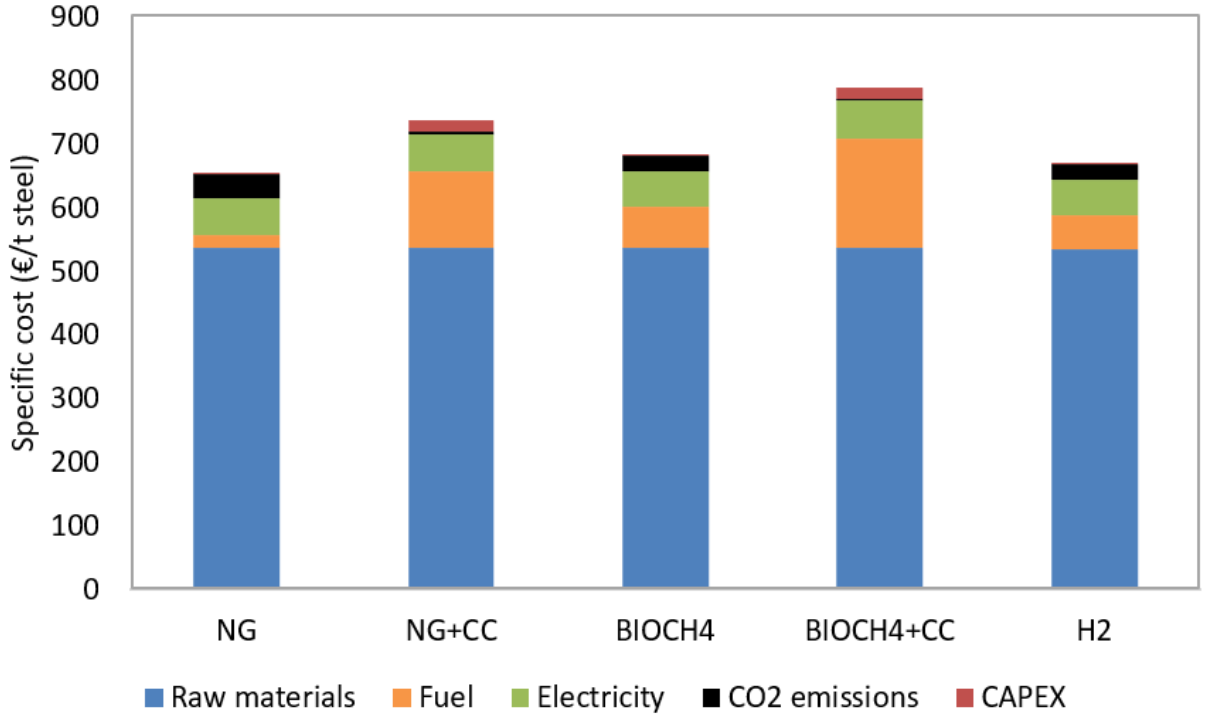

Figure 35: Cost breakdown of all cases in the competition pricing scenario

5.5 Identification of the best case

As the scope 1 and total CO_2 emissions as well as the cost for each case have been discussed in different scenarios, the Pareto plot, which is a comparative assessment of the cost and the emissions, can be presented for each pricing scenario discussed previously.

First, the Pareto plot related to the current 2026 price scenario and the 2026 emission factors is presented in Figure 36. As discussed above, the solutions that offer the best results in terms of emissions are both carbon capture alternatives, namely "NG+CC" and "BIOCH4+CC". The best overall case is the "BIOCH4" as its cost is the closest to the cheapest conventional "NG" case while still offering interesting emissions reduction. On the other hand, the "H2" configuration is the least attractive one, both from an economic and environmental point of view.

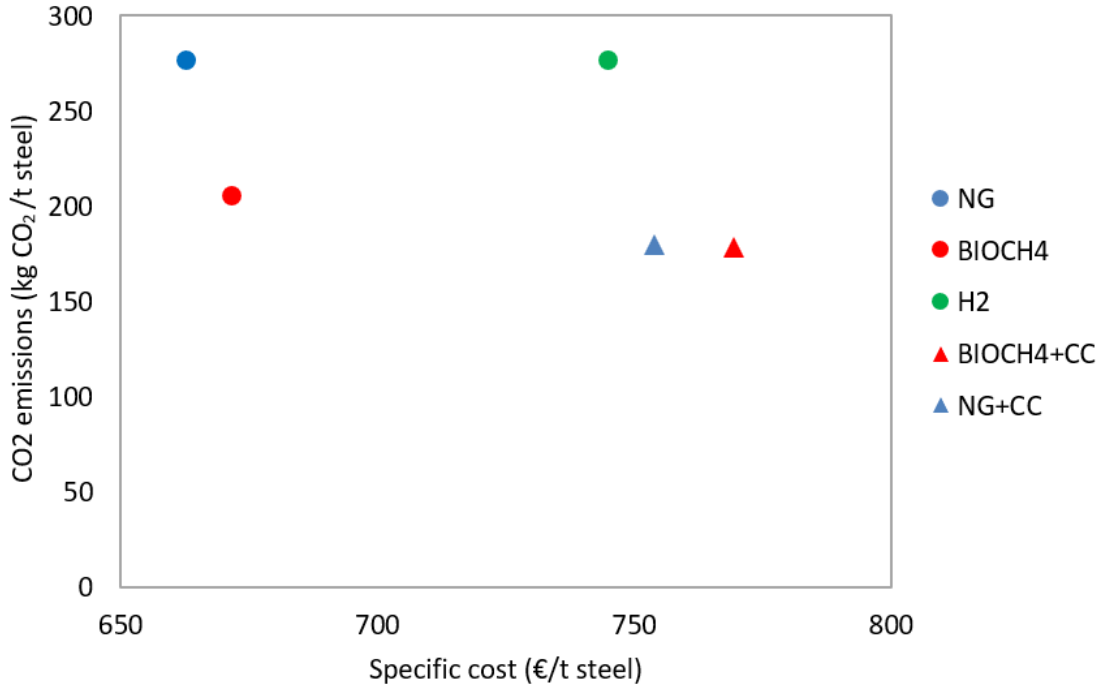

Figure 36: Specific total CO_2 emissions and specific cost for all cases in the 2026 pricing scenario

The comparative assessment in the ideal price scenario combined with the 2050 emission factors is depicted in Figure 37. It is clear that the "BIOCH4" remains the best alternative in this scenario, as it is associated with the lowest cost and the lowest total emissions. The "BIOCH4" configuration is closely followed by the "H2" case both in terms of cost and emissions, which provides an economic and environmental benefit compared to "NG". Finally, despite "NG+CC" and "BIOCH4+CC" being the least emitting options, their cost is too high compared to the other possibilities, rendering them not competitive.

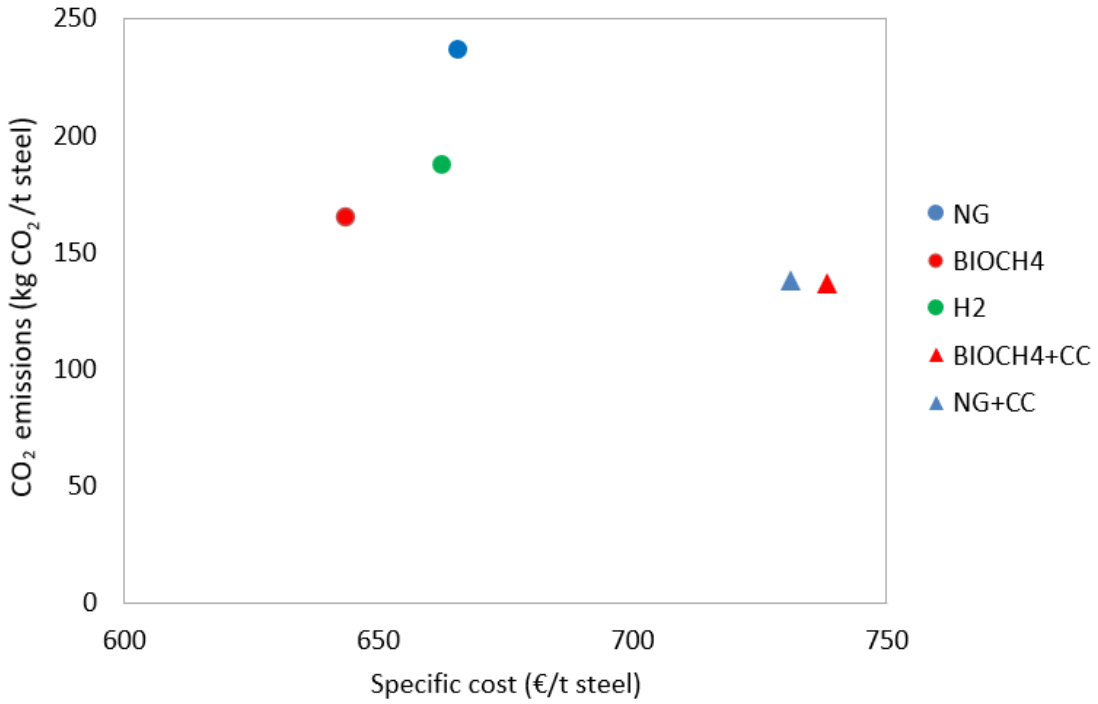

Figure 37: Specific total CO_2 emissions and specific cost for all cases in the ideal pricing scenario

Finally, Figure 38 represents the Pareto plot in the competition price scenario. With an increase in the price of biomethane, "BIOCH4" gets demoted to the third place in terms of price, while "BIOCH4+CC" becomes the most expensive alternative. The "NG" case becomes the cheapest again, with "H2" following it closely. Regarding the emissions, the discussion is the same than for the ideal scenario, as the same 2050 emission factors are also considered.

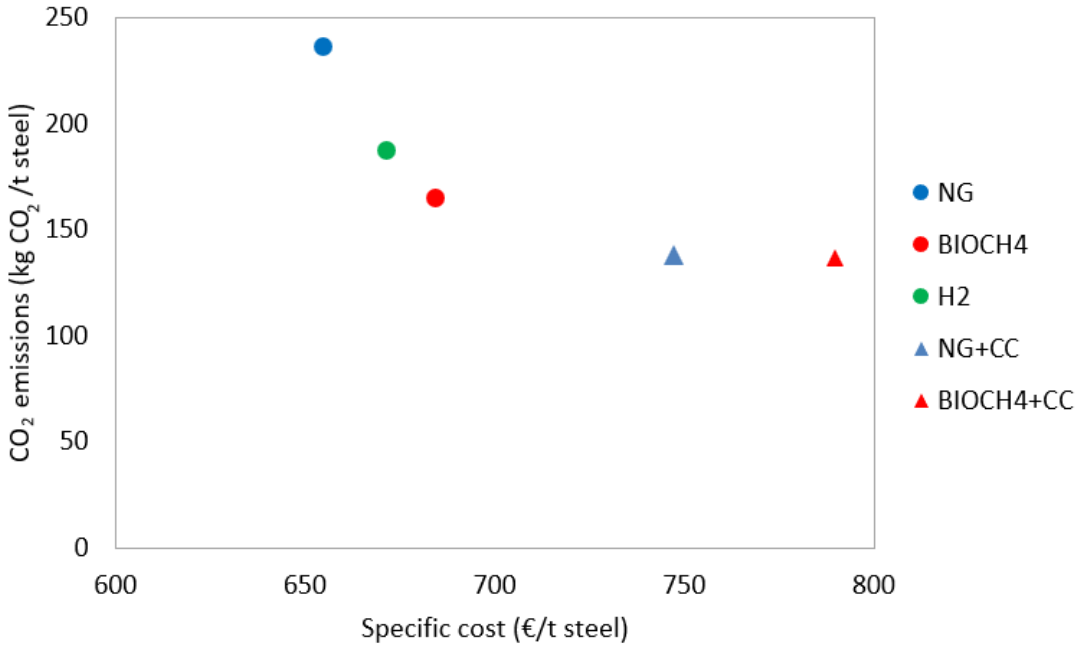

Figure 38: Specific total CO_2 emissions and specific cost for all cases in the competition pricing scenario

5.6 Final discussion

The model presents the biomethane as the best alternative fuel for the energy transition in the stainless steel industry. Without carbon capture, it is the closest transition to the current technology and with carbon capture, it is the solution that offers the biggest direct emissions reduction potential. However, it is important to note that, if biomethane is determined to be the best solution, its availability will become a critic factor in the transition choice. According to Fluxys [96], ten biomethane production units are operational today and around 20 are at the stage of research and development or construction. They predict that by 2040, the capacity of biomethane production could reach 15.6 TWh, which is approximatively 10% of the Belgian natural gas consumption. Hence, the stainless steel production plant modelled would use 7% of the biomethane available in Belgium. Even with rapid progress in the production, it is difficult to imagine that the Belgian biomethane production capacity will be sufficient to support the energy transition of multiple industrial sectors.

The results of this study showed that hydrogen is also an alternative that could get investigated but not necessary in the immediate future. In the current scenario, its high production cost makes it one of the more costly alternative. However, in the ideal and competition scenario, its more attractive price makes it closer to biomethane as an alternative, even overtaking it when biomass prices gets higher. A limitation to chose this solution could also be its availability. In 2024, hydrogen production in Belgium amounted to 20 000 TJ (around 555 GWh) and only 10% were from electricity [97]. Relating these values to the model, the stainless steel plant would consume 19.7% of the total yearly production, which is not a viable option. Progress in the availability and cost is very likely to happen but in the case of steel production with EAF, it should be better to investigate other alternatives

for the short term.

Even with a tax on CO_2 emissions, the cost associated to these emissions is still too small to push to invest into carbon capture technologies. In the 2026 scenario, it does not even represent 2% of the total cost in the "NG" case. In the ideal scenario, it represents a bigger part of the total cost but it has to be combined with low biomethane prices for the "BIOCH4" to become the most financially attractive configuration. In the competition case, when the price of biomethane is higher, the "NG" case remains the less expensive solution, despite an ETS price of 0.3€/kg CO_2.

Concerning the addition of a carbon capture unit, they are the better solutions if the focus is put on minimizing the emissions. However, their current high energy requirements in terms of fuel make them in the most expensive cases in every scenario considered. Progress in capture technologies are possible but there is still a long way to go before they come closer to the lower cost alternatives.

Finally, it is important to note that all the results obtained are dependant on assumptions about energy prices and production technologies, and how they will evolve. Being able to ideally predict how the energy market will behave is not easy and it has been proven again very recently. With the current conflict involving Middle Eastern countries that are major oil producers, the prices of fossil fuels have quickly increased and it is still difficult to predict how and when the market will evolve. Concerning renewable fuels, their use in big scale applications are still marginal because of the relatively low offer available. With more and more regulations at national and international levels, it is probably certain that greener technologies will become increasingly favourable but it is difficult to have an idea of when this change will operate.

6 Conclusions and perspectives

To be able to achieve the objectives of carbon neutrality by 2050 in Europe, major efforts still have to be done to decrease the emissions of CO_2. Industries that are high heat dependant will have the most difficulties to transition. The steelmaking industry which is part of it, has to massively invest in the transition of their process. While different steelmaking route exists, the BF-BOF route still represents the majority of steelmaking plant in the world.

The electric are furnace steelmaking route allows the use of recycled scrap as raw materials, improving its environmental impact compared other routes. To produce stainless steel, it requires three steps: the electric arc furnace, the argon-oxygen furnace as well as the the casting and rolling. In the EAF, scrap is melted with alloyed metals and mixed with oxygen and lime to remove impurities by oxidation. The AOD works under the same principle but requires more strict conditions such as inert gas injections to limit the oxidation and achieve the desired composition of steel. The final product of desired shape is obtained after the casting and the rolling, where the steel is first cooled and cut into shapes then reheated and rolled to form steel coil for example. Theses steps required high energy that is provided by electricity or natural gas combustion, resulting in elevated CO_2 emissions.

To improve the impact of the process, modification of the traditional process have been proposed. The switch of natural gas with greener fuel such as biomethane or hydrogen and the addition of a carbon capture unit have been considered. They have been modelled along side the natural gas based configuration by studying the required raw material and energy amount for each case and determine the CO_2 production. A cost analysis is also performed by considering the price of raw materials and fuels in different price scenarios. Additionally, the impact of the electricity and energy source on the process is also calculated.

According to the results, biomethane is a suitable alternative for natural gas as it allow great reduction in the scope 1 emissions and is the closest in total cost to the natural gas configuration, which is the cheapest in the 2026 scenario. When we consider a very low cost of biomass, it even become cheaper but this scenario is optimistic as an increase in price will be observed if the demand in biomethane increases.
While offering the best improvement in emission reductions, the addition of a carbon capture unit is the most expensive in all price scenarios as it suffers from a high fuel consumption. Green hydrogen offer similar results than biomethane in scope 1 but the scope 2 highly depends on the type of electricity that is used for its production. In the 2026 price scenario, its price is too expensive for it to be seriously invastigated but if it assumed that some will be imported at cheaper price than currently, it could become almost as interesting as biomethane

Even if this study is a good preliminary analysis on a few alternative pathways for the electric arc furnace route, some improvements could be brought to it. First, the addition of a heat integration inside the process could be explored. As off-gas at high temperature exits the EAF and AOD, it carries a great amount of heat that could be used to preheat the

raw materials or even to produce electricity that would be directly used. As an alternative type of charged material, DRI could be implemented in the model by using correlations that determined how the energy and raw materials demand evolve based on its proportion in replacing scrap. Multiple parameters relating to the provenance of the DRI and the method of production are making these correlations difficult to establish. In the existing model, the heat necessary for the desorption column of the carbon capture model is produced in a natural gas boiler. It could be improved by allowing the possibility to use biomethane, in particular for the "BIOCH4+CC".

Appendices

Numerical values of the figures of Section 5

Table A1: Indirect emissions for all cases in the 2026 scenario

kg CO_2/t steel	2026 grid	Solar panels	Onshore wind turbines
NG	85	62	25
NG+CC	158	134	95
BIOCH4	84	61	24
BIOCH4+CC	163	139	101
H2	156	133	96

Table A2: Total emissions breakdown for the 2026 scenario

kg CO_2/t steel	Scope 1	Scope 2 - Electricity	Scope 2 - Fuel
BASE CASE	191	70	15
BASE CASE+CC	22	73	85
BIOCH4	121	70	14
BIOCH4+CC	14	72	58
H2	121	70	86

Table A3: Indirect emissions for all cases in the 2050 scenario

kg CO_2/t steel	2050 grid	Solar panels	Wind turbines
NG	45	62	25
NG+CC	116	134	95
BIOCH4	44	61	14
BIOCH4+CC	121	139	101
H2	66	84	37

Table A4: Cost breakdown for all cases in the 2026 pricing scenario

€/t steel	NG	NG+CC	BIOCH4	BIOCH4+CC	H2
Raw materials	537	537	536	570	536
Fuel	19	103	33	126	106
Electricity	92	95	92	95	92
CO2 emission	14	2	9	1	9
CAPEX	2	17	2	18	3
Total	663	754	672	810	745

Table A5: Cost breakdown of all cases in the ideal pricing scenario

€/ t steel	NG	NG+CC	BIOCH4	BIOCH4+CC	H2
Raw materials	537	537	536	536	536
Fuel	22	120	21	129	39
Electricity	48	50	48	50	48
CO2 emissions	57	7	36	5	36
CAPEX	2	17	2	18	3
Total	666	731	644	738	662

Table A6: Cost breakdown of all cases in the competition pricing scenario

€/t steel	NG	NG+CC	BIOCH4	BIOCH4+CC	H2
Raw materials	537	537	536	536	536
Fuel	22	120	66	173	52
Electricity	56	58	56	59	56
CO2 emissions	38	4	24	3	24
CAPEX	2	17	2	18	3
Total	655	737	684	790	671

References

[1] United Nations Climate Change, *L'Accord de Paris*, Consulted on April 27th. [Online]. Available: https://unfccc.int/fr/a-propos-des-ndcs/l-accord-de-paris.

[2] *Émissions de gaz à effet de serre par pays et par secteur (infographie) | Thèmes | Parlement européen*. [Online]. Available: https://www.europarl.europa.eu/topics/fr/article/20180301STO98928/emissions-de-gaz-a-effet-de-serre-par-pays-et-par-secteur-infographie.

[3] A. Hüttel and J. Lehner, "Revisiting Investment Costs for Green Steel: Capital Expenditures, Firm Level Impacts, and Policy Implications," Tech. Rep.

[4] "World Steel in Figures," World Steel Association, Tech. Rep., 2025.

[5] World Steel Association, *World crude steel production from 2012 to 2024*. [Online]. Available: https://www.statista.com/statistics/267264/world-crude-steel-production/.

[6] S. Roudier et al., "Best available techniques (BAT) reference document for iron and steel production : industrial emissions Directive 2010/75/EU : integrated pollution prevention and control," Tech. Rep., 2013.

[7] M. A. Diez et al., "Coal use for iron and steel production in low-carbon transition scenarios," *The Coal Handbook: Volume 2: Towards Cleaner Coal Utilization, 2nd Edition*, vol. 2, pp. 493–546, Jan. 2023. doi: 10.1016/B978-0-12-824327-5.00010-7. [Online]. Available: https://www.sciencedirect.com/science/chapter/edited-volume/pii/B9780128243275000107.

[8] *Smelting reduction process - Global Energy Monitor*. [Online]. Available: https://www.gem.wiki/Smelting_reduction_process.

[9] M. Rumsa et al., "Global steel decarbonisation roadmaps: Near-zero by 2050," *Environmental Impact Assessment Review*, vol. 112, Mar. 2025. doi: 10.1016/j.eiar.2025.107807.

[10] M. Kovačič et al., "Comprehensive electric arc furnace electric energy consumption modeling: A pilot study," *Energies*, vol. 12, no. 11, Jun. 2019. doi: 10.3390/en12112142.

[11] M. M. Abadi et al., *A review of simulation and numerical modeling of electric arc furnace (EAF) and its processes*, Jun. 2024. doi: 10.1016/j.heliyon.2024.e32157.

[12] T. S. Kho et al., "Understanding stainless steelmaking through computational thermodynamics part 1: Electric arc furnace melting," *Transactions of the Institutions of Mining and Metallurgy, Section C: Mineral Processing and Extractive Metallurgy*, vol. 119, no. 1, pp. 1–8, 2010. doi: 10.1179/174328509X431454.

[13] H. J. Odenthal et al., "Review on Modeling and Simulation of the Electric Arc Furnace (EAF)," *Steel Research International*, vol. 89, no. 1, Jan. 2018. doi: 10.1002/srin.201700098.

[14] C. Schubert et al., "Development of a fast modeling approach for the prediction of scrap preheating in continuously charged metallurgical recycling processes," *Metals*, vol. 11, no. 8, p. 1280, Aug. 2021. doi: 10.3390/met11081280. [Online]. Available: http://dx.doi.org/10.3390/met11081280.

[15] M. Tunc et al., "Energy Analysis of the Operation of an Electric-Arc Furnace at a Steel Company in Turkey," *Metallurgist*, vol. 59, no. 5-6, pp. 489–497, Sep. 2015. doi: 10.1007/s11015-015-0130-5.

[16] R. D. MacRosty and C. L. Swartz, "Dynamic modeling of an industrial electric arc furnace," *Industrial and Engineering Chemistry Research*, vol. 44, no. 21, pp. 8067–8083, Oct. 2005. doi: 10.1021/ie050101b.

[17] M. Kirschen et al., "Energy efficiency and the influence of gas burners to the energy related carbon dioxide emissions of electric arc furnaces in steel industry," *Energy*, vol. 34, no. 9, pp. 1065–1072, 2009. doi: 10.1016/j.energy.2009.04.015.

[18] J. Reichel et al., "EAF-foamy slag in stainless steel production new extremely efficient technology easy to handle and cost-efficient," *Archives of Metallurgy and Materials*, 2008.

[19] "Fiche technique acier 314," [Online]. Available: https://www.agst-steel.de/nuances/AISI_314_1.4841.pdf.

[20] D. R. Swinbourne et al., "Understanding stainless steelmaking through computational thermodynamics: Part 3 - AOD converting," *Transactions of the Institutions of Mining and Metallurgy, Section C: Mineral Processing and Extractive Metallurgy*, vol. 121, no. 1, pp. 23–31, 2012. doi: 10.1179/1743285511Y.0000000031.

[21] D. R. Swinbourne et al., "Understanding stainless steelmaking through computational thermodynamics Part 2 - VOD converting," *Transactions of the Institutions of Mining and Metallurgy, Section C: Mineral Processing and Extractive Metallurgy*, vol. 119, no. 2, pp. 107–115, Jun. 2010. doi: 10.1179/174328509X481909.

[22] P. Singha, "Refining Contribution at Hotspot and Emulsion Zones of Argon Oxygen Decarburization: Fundamental Analysis Based upon the FactSage-Macro Program Approach," *Metallurgical and Materials Transactions B: Process Metallurgy and Materials Processing Science*, vol. 55, no. 4, pp. 2181–2193, Aug. 2024. doi: 10.1007/s11663-024-03084-4.

[23] P.-J. Cunat, "Affinage des aciers inoxydables," *Matériaux | Élaboration et recyclage des métaux*, 2008.

[24] V. V. Visuri et al., "A mathematical model for the reduction stage of the AOD process. Part I: Derivation of the model," *ISIJ International*, vol. 53, no. 4, pp. 603–612, 2013. doi: 10.2355/isijinternational.53.603.

[25] *What is steel and how is steel made?* [Online]. Available: https://www.eurofer.eu/about-steel/learn-about-steel/what-is-steel-and-how-is-steel-made.

[26] H. Guo et al., "Dynamic fuel optimization and environmental-economic trade-offs in steel rolling heating furnaces: a multi-objective analysis of biogas-natural gas substitution," *Applied Thermal Engineering*, vol. 284, Jan. 2026. doi: 10.1016/j.applthermaleng.2025.128939.

[27] Y. Khalid et al., "Oxygen enrichment combustion to reduce fossil energy consumption and emissions in hot rolling steel production," *Journal of Cleaner Production*, vol. 320, Oct. 2021. doi: 10.1016/j.jclepro.2021.128714.

[28] T. Steinparzer et al., "Electric arc furnace off-gas heat recovery and experience with a testing plant," *Steel Research International*, vol. 85, no. 4, pp. 519–526, Apr. 2014. doi: 10.1002/srin.201300228.

[29] G. Hartfuß et al., "Off-Gas Waste Heat Recovery for Electric Arc Furnace Steelmaking Using Calcium Hydroxide (Ca(OH)2) Dehydration," *Steel Research International*, vol. 91, no. 11, Nov. 2020. doi: 10.1002/srin.202000048.

[30] E. Rudnik, *Hydrometallurgical Treatment of EAF By-Products for Metal Recovery: Opportunities and Challenges*, Aug. 2025. doi: 10.3390/met15080914.

[31] M. D. Godson et al., "Electric arc furnace slag - A prospective alternative for railway sub-ballast layer," *Construction and Building Materials*, vol. 483, Jul. 2025. doi: 10.1016/j.conbuildmat.2025.141702.

[32] K. Kanon et al., "Optimization of Process Parameters for Sustainable Electric Arc Furnace Steel Slag Reinforced Glass Fiber–Epoxy Composites for X-Ray Shielding," *Polymers for Advanced Technologies*, vol. 36, no. 10, Oct. 2025. doi: 10.1002/pat.70373.

[33] S. Radić et al., "Recycling Electric Arc Furnace Slag into Fertilizer: Effects of "Waste Product" on Growth and Physiology of the Common Bean (Phaseolus vulgaris L.)," *Agronomy*, vol. 12, no. 9, Sep. 2022. doi: 10.3390/agronomy12092218.

[34] M. De Colle et al., "The use of high-alloyed EAF slag for the neutralization of on-site produced acidic wastewater: The first step towards a zero-waste stainless-steel production process," *Applied Sciences (Switzerland)*, vol. 9, no. 19, Oct. 2019. doi: 10.3390/app9193974.

[35] L. Mo, "Carbon dioxide sequestration on steel slag," in *Carbon Dioxide Sequestration in Cementitious Construction Materials*, Elsevier, Jan. 2018, pp. 175–197. doi: 10.1016/B978-0-08-102444-7.00008-3.

[36] H. W. Li et al., "A novel method to enhance polychlorinated dibenzo-p-dioxins and dibenzofurans removal by adding bio-solution in EAF dust treatment plant," *Journal of Hazardous Materials*, vol. 150, no. 1, pp. 83–91, Jan. 2008. doi: 10.1016/j.jhazmat.2007.04.077.

[37] M. Kamali et al., "Magnetic MgFe2O4–CaFe2O4 S-scheme photocatalyst prepared from recycling of electric arc furnace dust," *Journal of Environmental Management*, vol. 290, Jul. 2021. doi: 10.1016/j.jenvman.2021.112609.

[38] A. Lozano-Lunar et al., "Safe use of electric arc furnace dust as secondary raw material in self-compacting mortars production," *Journal of Cleaner Production*, vol. 211, pp. 1375–1388, Feb. 2019. doi: 10.1016/j.jclepro.2018.12.002.

[39] N. Antuñano et al., *Hydrometallurgical processes for Waelz oxide valorisation – An overview*, Sep. 2019. doi: 10.1016/j.psep.2019.06.028.

[40] P. Liptai et al., "Hydrometallurgical Recycling of Electric Arc Furnace Dust: Application Possibilities of ZnO Product for the Manufacture of Varistors in the Electrotechnical Industry," *Waste and Biomass Valorization*, vol. 11, no. 8, pp. 4419–4428, Aug. 2020. doi: 10.1007/s12649-019-00722-w.

[41] A. N. Conejo et al., "Recycling MgO-C refractory in electric arc furnaces," *Resources, Conservation and Recycling*, vol. 49, no. 1, pp. 14–31, Nov. 2006. doi: 10.1016/j.resconrec.2006.03.002.

[42] World Steel Association, *Average carbon dioxide (CO2) emissions intensity of steel production worldwide from 2021 to 2023, by production route (in metric tons of CO2 per metric ton of crude steel)*, 2024. [Online]. Available: https://www.statista.com/statistics/1446819/steel-emissions-intensity-by-production-route/.

[43] B. Xue et al., "Analysis of energy consumption and carbon emissions of electric arc furnace steelmaking using hydrogen-based direct reduced iron," *Process Safety and Environmental Protection*, vol. 201, Sep. 2025. doi: 10.1016/j.psep.2025.107617.

[44] M. A. Elkader et al., "Influence of direct-reduced iron percentage in EAF charge mix on EAF operation parameters," *Steel Grips*, 2015.

[45] N. Arzpeyma et al., "Development of a mass and energy balance model and its application for HBI charged eafs," *Metals*, vol. 10, no. 3, Mar. 2020. doi: 10.3390/met10030311.

[46] *Biomethane, a game changer for the steel industry's decarbonization efforts*. [Online]. Available: https://www.expometals.net/en/news/biomethane-a-game-changer-for-the-steel-industrys-decarbonization-efforts.

[47] *Ternium: Natural gas replacement by the use of biomethane from a landfill at stationary combustion sources - worldsteel.org*. [Online]. Available: https://worldsteel.org/case-studies/sustainability/natural-gas-replacement-by-the-use-of-biomethane-from-a-landfill-at-stationary-combustion-sources/.

[48] B. Xue et al., "A case study on biomass steelmaking in electric arc furnaces: Mass, energy and emission analysis," *Ironmaking and Steelmaking*, 2026. doi: 10.1177/03019233261429765.

[49] *Les types d'hydrogène et leurs modalités de production*. [Online]. Available: https://www.lunil.com/les-types-dhydrogene-et-leurs-modalites-de-production/.

[50] *Higher Calorific Values of Common Fuels: Reference & Data*. [Online]. Available: https://www.engineeringtoolbox.com/fuels-higher-calorific-values-d_169.html.

[51] A. Della Rocca et al., "Rolling mill decarbonization: Tenova SmartBurners with 100% hydrogen," *Materiaux et Techniques*, vol. 109, no. 3-4, 2021. doi: 10.1051/mattech/2022012.

[52] *World's first fossil-free hydrogen plant revolutionizes steel - Ovako*. [Online]. Available: https://www.ovako.com/en/about-ovako/worlds-first-fossil-free-hydrogen-plant-for-steel-heating.

[53] F. Meng et al., "Research progress of aqueous amine solution for co2 capture: A review," *Renewable and Sustainable Energy Reviews*, vol. 168, p. 112 902, Oct. 2022. doi: 10.1016/j.rser.2022.112902. [Online]. Available: http://dx.doi.org/10.1016/j.rser.2022.112902.

[54] F. Raganati and P. Ammendola, *CO2 Post-combustion Capture: A Critical Review of Current Technologies and Future Directions*, Aug. 2024. doi: 10.1021/acs.energyfuels.4c02513.

[55] M. Erans et al., "Calcium looping sorbents for co2 capture," *Applied Energy*, vol. 180, pp. 722–742, Oct. 2016. doi: 10.1016/j.apenergy.2016.07.074. [Online]. Available: http://dx.doi.org/10.1016/j.apenergy.2016.07.074.

[56] M. M. F. Hasan et al., "Modeling, simulation, and optimization of postcombustion co₂capture for variable feed concentration and flow rate. 2. pressure swing adsorption and vacuum swing adsorption processes," *Industrial amp; Engineering Chemistry Research*, vol. 51, no. 48, pp. 15 665–15 682, Nov. 2012. doi: 10.1021/ie301572n. [Online]. Available: http://dx.doi.org/10.1021/ie301572n.

[57] R. Mitraki, "Transition pathways for the Belgian Industry: application to the case of the lime sector," Ph.D. dissertation, 2024. [Online]. Available: https://lib.uliege.behttps://matheo.uliege.be.

[58] APERAM, "APERAM CHÂTELET brochure," Tech. Rep., 2023. [Online]. Available: www.aperamchatelet.be.

[59] *[EPOS] Osmose presentation - YouTube*. [Online]. Available: https://www.youtube.com/watch?v=atK5dZAjiEA&t=2724s.

[60] M. Kirschen et al., "MASS AND ENERGY BALANCES OF STAINLESS STEEL EAF," 2002.

[61] B. Tian et al., "A Static Balance Model and Analysis of 430 Stainless Steel Produced by Basic Oxygen Furnace–Argon Oxygen Decarburization Furnace Process," *Steel Research International*, vol. 93, no. 7, Jul. 2022. doi: 10.1002/srin.202100852.

[62] G. Zabik et al., "Hydrogen and Synthetic Natural Gas for decarbonizing steel hot rolling mills: Economic viability under dynamic electricity pricing," *Energy Conversion and Management*, vol. 341, Oct. 2025. doi: 10.1016/j.enconman.2025.119912.

[63] S. m. Kim and G. Léonard, "CO2 capture technologies and shortcut cost correlations for different inlet CO2 concentrations and flow rates. part 1: Chemical absorption," *International Journal of Greenhouse Gas Control*, vol. 145, p. 104 391, Jul. 2025. doi: 10.1016/J.IJGGC.2025.104391. [Online]. Available: https://www.sciencedirect.com/science/article/pii/S1750583625000891.

[64] S. Lyons et al., "Industrial Fuel Switching Market Engagement Study," Business, Energy & Industrial Department, Tech. Rep., Dec. 2018. [Online]. Available: https://www.aperamchatelet.be/fr/espace-presse/.

[65] *Scrap Steel - Price - Chart - Historical Data - News*, Consulted on May 5th. [Online]. Available: https://tradingeconomics.com/commodity/scrap-steel.

[66] *Quicklime Prices: Key Price Trend 2025 & Forecast Data – Chemical Industry Pricing Reports*, Consulted on May 5th. [Online]. Available: https://chemicalindustrypricingreports.wordpress.com/2025/04/02/quicklime-prices-key-price-trend-2025-forecast-data/.

[67] *Ferroalloys Prices - Current & Historial Prices, Charts, Export Prices from China, Europe, USA, India and South Africa | ScrapMonster*, Consulted on May 5th. [Online]. Available: https://www.scrapmonster.com/metal-prices/ferroalloys.

[68] *Oxygen Prices 2026 | May Price Chart, Trend & Forecast*, Consulted on May 5th. [Online]. Available: https://www.imarcgroup.com/oxygen-pricing-report.

[69] *Argon Prices 2026 | May Price Chart & Index, Forecast*, Consulted on May 5th. [Online]. Available: https://www.imarcgroup.com/argon-pricing-report.

[70] *Nitrogen Prices 2026 | May Price Chart & Index, Forecast*, Consulted on May 5th. [Online]. Available: https://www.imarcgroup.com/nitrogen-pricing-report.

[71] *Natural gas price statistics - Statistics Explained - Eurostat*. [Online]. Available: https://ec.europa.eu/eurostat/statistics-explained/index.php?title=Natural_gas_price_statistics.

[72] BIP Europe, "Insights into the current cost of biomethane production from real industry data," 2023.

[73] *Cost of hydrogen production | European Hydrogen Observatory*, Consulted on May 5th. [Online]. Available: https://observatory.clean-hydrogen.europa.eu/index.php/hydrogen-landscape/production-trade-and-cost/cost-hydrogen-production.

[74] *Electricity price statistics - Statistics Explained - Eurostat*, Consulted on May 15th. [Online]. Available: https://ec.europa.eu/eurostat/statistics-explained/index.php?title=Electricity_price_statistics.

[75] *EU Carbon Permits - Price - Chart - Historical Data - News*, Consulted on May 15th. [Online]. Available: https://tradingeconomics.com/commodity/carbon.

[76] R. Mitraki et al., "Evaluation of energy transition pathways for the instant coffee industry," *Submitted for publication*, 2026, Under review.

[77] Elia, "Belgian electricity system blueprint for 2035-2050," Tech. Rep., 2024. [Online]. Available: https://issuu.com/eliagroup/docs/20240924_belgianelectricitysystemblue 205.

[78] EnergyVille, *PATHS2050 | Main edition 2025 - Assumptions*, 2025. [Online]. Available: https://perspective2050.energyville.be/results/main-edition-2025/assumptions.

[79] Material Economics, "EU Biomass Use in a Net-Zero Economy: A course correction for EU biomass," Tech. Rep., 2021, Consulted on May 15th. [Online]. Available: https://materialeconomics.com/node/3.

[80] *Belgium: power sector carbon intensity 2023| Statista*. [Online]. Available: https://www.statista.com/statistics/1290132/carbon-intensity-power-sector-belgium/.

[81] *ENTSO-E and ENTSOG TYNDP 2024 Draft Scenarios Report*, Consulted on May 15th. [Online]. Available: https://2024.entsos-tyndp-scenarios.eu/#download.

[82] *electricity production, wind, 1-3MW turbine, onshore - Belgium - electricity, high voltage | ecoQuery*, Consulted on May 15th. [Online]. Available: https://ecoquery.ecoinvent.org/3.12/cutoff/dataset/534/documentation.

[83] *electricity production, wind, >3MW turbine, onshore - Belgium - electricity, high voltage | ecoQuery*, Consulted on May 15th. [Online]. Available: https://ecoquery.ecoinvent.org/3.12/cutoff/dataset/4409/documentation.

[84] *electricity production, wind, 1-3MW turbine, offshore - Belgium - electricity, high voltage | ecoQuery*, Consulted on May 15th. [Online]. Available: https://ecoquery.ecoinvent.org/3.12/cutoff/dataset/2945/documentation.

[85] *electricity production, photovoltaic, 3kWp slanted-roof installation, multi-Si, panel, mounted - Belgium - electricity, low voltage | ecoQuery*, Consulted on May 15th. [Online]. Available: https://ecoquery.ecoinvent.org/3.12/cutoff/dataset/6696/documentation.

[86] *electricity production, photovoltaic, 3kWp slanted-roof installation, single-Si, panel, mounted - Belgium - electricity, low voltage | ecoQuery*, Consulted on May 15th. [Online]. Available: https://ecoquery.ecoinvent.org/3.12/cutoff/dataset/8058/documentation.

[87] *electricity production, photovoltaic, 570kWp open ground installation, multi-Si - Belgium - electricity, low voltage | ecoQuery*, Consulted on May 15th. [Online]. Available: https://ecoquery.ecoinvent.org/3.12/cutoff/dataset/16924/documentation.

[88] *electricity production, deep geothermal - France - electricity, high voltage | ecoQuery*, Consulted on May 15th. [Online]. Available: https://ecoquery.ecoinvent.org/3.12/cutoff/dataset/16345/documentation.

[89] *electricity production, hydro, pumped storage - Belgium - electricity, high voltage | ecoQuery*, Consulted on May 15th. [Online]. Available: https://ecoquery.ecoinvent.org/3.12/cutoff/dataset/1553/documentation.

[90] *electricity production, nuclear, pressure water reactor - Belgium - electricity, high voltage | ecoQuery*, Consulted on May 15th. [Online]. Available: https://ecoquery.ecoinvent.org/3.12/cutoff/dataset/8228/documentation.

[91] *electricity production, natural gas, conventional power plant - Belgium - electricity, high voltage | ecoQuery*, Consulted on May 15th. [Online]. Available: https://ecoquery.ecoinvent.org/3.12/cutoff/dataset/4943/documentation.

[92] *electricity production, natural gas, combined cycle power plant - Belgium - electricity, high voltage | ecoQuery*, Consulted on May 15th. [Online]. Available: https://ecoquery.ecoinvent.org/3.12/cutoff/dataset/12705/documentation.

[93] *heat and power co-generation, natural gas, combined cycle power plant, 400MW electrical - Belgium - electricity, high voltage | ecoQuery*, Consulted on May 15th. [Online]. Available: https://ecoquery.ecoinvent.org/3.12/cutoff/dataset/13768/documentation.

[94] *heat and power co-generation, natural gas, conventional power plant, 100MW electrical - Belgium - electricity, high voltage | ecoQuery*, Consulted on May 15th. [Online]. Available: https://ecoquery.ecoinvent.org/3.12/cutoff/dataset/13289/documentation.

[95] N. Tenhumberg and K. Büker, "Ecological and economic evaluation of hydrogen production by different water electrolysis technologies," *Chemie Ingenieur Technik*, vol. 92, no. 10, pp. 1586–1595, Aug. 2020. doi: 10.1002/cite.202000090. [Online]. Available: http://dx.doi.org/10.1002/cite.202000090.

[96] Fluxys, *Biomethane: a local, green and quick-fit solution*. [Online]. Available: https://www.fluxys.com/en/natural-gas-and-biomethane/what-is-biomethane.

[97] *Consultez les derniers chiffres sur l'énergie en Belgique | SPF Economie*. [Online]. Available: https://economie.fgov.be/fr/nouveautes/consultez-les-derniers.